SYNTHESIS OF NOVEL FENARIMOL ANALOGUES AS DRUG CANDIDATES FOR THE NEGLECTED TROPICAL DISEASE MYCETOMA

HUNG PHAT DUONG

A thesis submitted in partial fulfilment of the requirements for the degree of Bachelor of Science (Honours)

NOVEMBER 2017

Abstract

Mycetoma is a type of skin infection caused by bacteria and fungi, characterised by skin lesions with granular discharge. This disease mainly affects people in poor communities with limited health education. There is currently no effective affordable treatment for mycetoma and this disease may cause gradual disfigurement over many years, with amputation as an eventual certainty.

In 2016, the Drug for Neglected Diseases initiative started the first clinical trial for mycetoma. Yet beyond that there exists no other drug candidates against mycetoma. The lack of financial returns means that support for research from the private sector is minimal. It was amidst these hopeless circumstances that the present project was conceived.

Screening of a diverse range of drug-like molecules against *Madurella Mycetomatis*, the main pathogen of fungal mycetoma, showed the fenarimol analogues as promising candidates against mycetoma, with a high potency, a public domain status and a diverse library of analogues. The present project set out to resynthesise the initial potent fenarimol analogues to confirm a viable synthetic route and reassert the accuracy of the initial potency. Guided by the biological evaluation results, novel fenarimol analogues were synthesised that serve to explore chemical moieties associated with high potency.

The preliminary result revealed some chemical moieties to be more active against mycetoma than others. For instance, the removal of a single fluoro- group correlated to a drastic reduction in activity while the change of a bromo- to a nitrile- group saw little change in activity. Perhaps the biggest challenge in the present project is the ability of fungal mycetoma to exclusively form protective grains in living organisms which are impervious to many otherwise potent drugs such that some best *in vitro* compounds were rendered useless in the *in vivo* model.

However, a correlation in lipophilicity and *in vivo* activity means that the grains composition was one step closer to being elucidated. Future synthesis can also be optimised to have lower lipophilicity to improve *in vivo* potency.

The present project also adopted an open source approach where research data are in the public domain and the general communities are encouraged to input ideas to fast track drug discovery. Such an open source framework means that the results obtained from this project will benefit those who need help the most: the patients of mycetoma.

Statement of Student Contributions

This project was provided by A/Prof Matthew Todd. The open source approach to this project was initiated by A/Prof Todd. The initial potent compounds against mycetoma were identified by Dr. Wendy van de Sande and her team at the Department of Medical Microbiology and Infectious Diseases, Erasmus University, Rotterdam, the Netherlands, and a team including Benjamin Perry and Jean-Robert Ioset at the Drugs for Neglected Diseases Initiative (DNDi), Geneva. The direction of novel synthesis was chosen by me after discussions with A/Prof Todd, Dr. Malcolm Spain and Mr. Edwin Tse.

Unless otherwise specified, all chemical synthesis in the present thesis was performed by me with initial guidance by Dr. Alice Williamson, Dr. Malcolm Spain and Mr. Edwin Tse.

Nuclear magnetic resonance (NMR) spectroscopy was carried out by me with initial help from Dr. Alice Williamson, Mr. Edwin Tse and Dr. Malcolm Spain, or was performed by Dr. Ian Luck and associates at the School of Chemistry's NMR Facility, University of Sydney.

Low resolution mass spectrometry was performed in part by me with initial help from Dr. Nick Proschogo. Low resolution and high resolution mass spectrometry were also performed by Dr. Nick Proschogo and associates at the School of Chemistry's Mass Spectrometry Facility, University of Sydney.

Elemental microanalysis was performed by Dr. Peter Karuso and associates at the Microanalysis Facility, Department of Chemistry and Biomolecular Sciences, Macquarie University.

Other spectroscopic analysis (such as infrared and melting points) were carried out by me. All spectroscopic data were analysed by me with occasional inputs from Mr. Edwin Tse, Dr. Malcolm Spain and A/Prof Matthew Todd.

Biological evaluation was performed by Dr. Wendy van de Sande and her research team, using chemicals synthesised by me, provided by Dr. Perry (DNDi) and originating from their chemical library at Epichem (Perth), or provided by

Medicines for Malaria Venture Pathogen Box. Analysis of biological evaluation results was performed by me and A/Prof Todd, in collaboration with Dr. van de Sande and Dr. Perry. The lipophilicity correlation was discovered by Dr. Perry.

Proofreading of this thesis was performed by A/Prof Todd, Mr. Edwin Tse, Mr. James Batten and Ms. Nicole Groves from the University of Sydney, and Mr. Trung Hieu Bui from Macquarie University.

I certify that this report contains work carried out by me

except where otherwise acknowledged.

Hung Phat Duong

5th November 2017

Acknowledgement

To A/Prof Todd for giving me the opportunities to work in your group, for your vast knowledge and expertise which you are always happy to share with me, for leadership and guidance and for always believing in me.

To A/Prof Rutledge for being my unofficial second supervisor and for always guiding me to think critically as a chemist.

To Malcolm and Edwin for always going out of your way to help me when I am in troubles. You help me become a better chemist and a better person.

To my peers, Conor, Seb and Jack for your unwavering support and company. My year has been made brighter by your presence.

To everyone in the Todd-Rutledge group for always looking out for me and each other, making sure that everything is always safe, nice and neat. And most importantly, fun!

To my family for your love and support. Few words can describe how much you mean to me.

To my best friend Hieu for always being there for me when I need you.

Table of Contents

List of Abbreviations

Boc	tert-butyloxycarbonyl
br	broad
d	doublet
DCM	dichloromethane
dd	doublet of doublets
ddd	doublet of doublets of doublets
DMA	dimethylacetamide
DMSO	dimethylsulfoxide
DND*i*	Drugs for Neglected Diseases initiative
dt	doublet of triplets
equiv	equivalent
h	hour(s)
IC	inhibitory concentration
M	molar
m	multiplet
MIC	minimum inhibitory concentration
min	minutes

mol	mole(s)
NMR	nuclear magnetic resonance
NTD	Neglected Tropical Disease
q	quartet
rt	room temperature
s	(for IR) strong
s	(for NMR) singlet
S_N1	uniolecular nucleophilic substitution
S_N2	bimolecular nucleophilic substitution
t	triplet
tdd	triplet of doublets of doublets
TFA	trifluoroacetic acid
THF	tetrahydrofuran
TLC	thin layer chhromatography
UV	ultraviolet
w	weak
WHO	World Health Organisation

Chapter 1: Introduction

1.1. What is Mycetoma?

Figure 1: Foot deformity caused by mycetoma.[1] Reproduced with permission from the original CC BY-NC-SA 3.0 CH licence

Mycetoma is an infection characterised by subcutaneous masses and sinuses with granular discharge (**Figure 1**).[2] The disease starts when the causative organisms enter the skin through openings from injuries such as a thorn prick.[3] Despite the painless initial stage, the infection progressively deepens towards nerves and bones over many years, causing pain and making treatment difficult. Mycetoma may spread *via* the circulatory and lymphatic systems, resulting in metastasis.[4-5]

On 28 May 2016, the World Health Organisation (WHO) officially recognised mycetoma as the latest of 18 neglected tropical diseases (NTDs).[6] Like other NTDs, mycetoma mainly affects impoverished communities in developing countries where health education was limited. Mycetoma is prevalent in tropical and subtropical areas between the latitudes 30° north and 15° south, which include countries such as Mexico, Brazil, Sudan, Somalia and India.[2] The incidence rates of mycetoma in Mexico and Sudan are 0.15 and 1.81 cases per 100,000 people respectively.[7] Over the past 54 years, nearly 4,000 cases of mycetoma were documented in Mexico.[8] More than 7,000 cases of mycetoma have been treated at the Mycetoma Research Centre in Khartoum, Sudan.[2] However, these numbers are a gross underestimation of the disease's prevalence because basic knowledge about the epidemiology of mycetoma is limited, which hinders the development of accurate prevalence statistics.

There are two types of mycetoma: actinomycetoma caused by bacterial infection and eumycetoma caused by fungal infection. Actinomycetoma is most prevalent in Mexico and eumycetoma is most prevalent in Sudan.[2] Actinomycetoma is more aggressive but can be effectively treated with a course of antibiotics (90% curative rate). Although eumycetoma is more progressive, antifungal treatment is less effective (25–35% curative rate). The long-term ineffective mycetoma treatment involves toxic drugs with no better alternatives: ketoconazole is restricted due to severe side effects whereas itraconazole only treats the symptoms of the disease.[10-11] Surgery and amputation are common last-resort treatments for eumycetoma and even these extreme measures do not guarantee success.

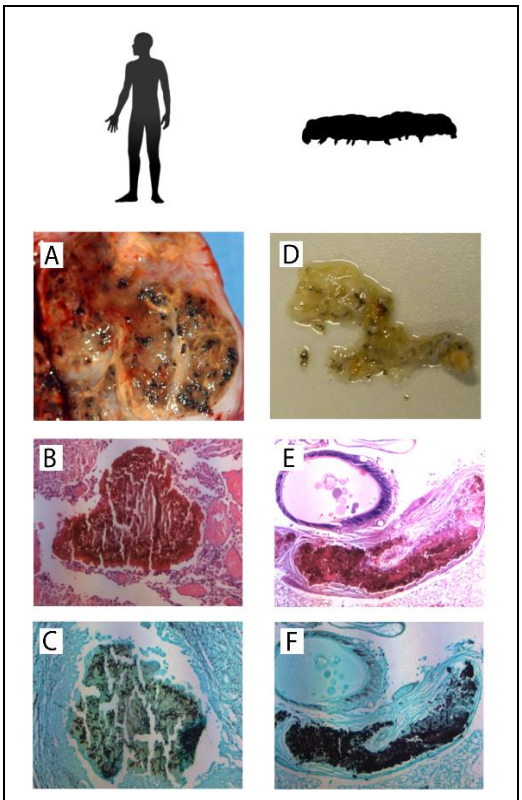

Figure 2: Eumycetoma in human (A–C) and larval (D–F) tissues. Grain formation appear as black aggregates (A and D). Grains are also apparent in HE stained slides (100× times magnified) as black dots (B and E). The presence of the fungus is shown as black dendritic patterns (hyphae) on Grocott stained slides (100× times magnified) (C and F).[9] Reproduced with permission from original CC-BY-4.0 licence.

1.2. Challenges in Drug Discovery for Eumycetoma

Treatment of eumycetoma can be ineffective because of fibrous granular formations surrounding the infection sites that lower the immune response's efficiency and hinder drug penetration (**Figure 2**, A–C).[2, 12] Development of drugs to target eumycetoma faces the same problem. Dr. Wendy van de Sande, a collaborator of the present project, developed the first *in vivo* assay for *Madullera mycetomatis*, the most common causative fungus of eumycetoma.[9] Dr. van de Sande is one of the pioneers in mycetoma research and a founding member of the Mycetoma Consortium which successfully advocated for mycetoma to be recognised as a NTD by WHO. Her assay uses larvae of the wax

moth *Galleria mellonella* and successfully recreate grain formation inside the larval model.[9] *G. mellonella* larvae were chosen because they are easy to care for and manipulate.[9] These larvae produce neutrophils which are also found in humans and are believed to facilitate grain formation.[9] *G. mellonella* larvae have an innate immune system like humans and can be kept at body temperature.[9] These features make *G. mellonella* larva a perfect *in vivo* assay for eumycetoma.

The current *in vitro* assays for eumycetoma do not replicate such grain formation (**Figure 2**, D–F). This limitation means that even though the *in vitro* assays may produce promising preliminary results in a fast and efficient manner, those results may not translate to good *in vivo* activity if the drug cannot pass the granular barrier in a living organism to target the pathogen, which is the ultimate goal. Research is ongoing to uncover the identity of the constituents of the grains as well as to create an *in vitro* assay for eumycetoma grain penetration by small molecules.

1.3. Patients of Eumycetoma

Patients suffer from eumycetoma on many levels: physically, financially and socially. In endemic areas, field-working young people are more exposed to infested soil and prone to injuries from physical labour. The painless but persistent eumycetoma progressively disfigures once-healthy bread winners, turning them into the dependent in their families, furthering their financial burden.[13] These patients avoid professional treatments due to the scarcity of medical clinics, fear of amputation and social stigma. They only come to seek help when the infection advances to the painful stage, the point at which antifungal treatment is less effective and amputations are certain. The long duration, high cost and ineffectiveness of eumycetoma treatments are so discouraging to patients that they often turn to traditional medicine, which only worsens their conditions.

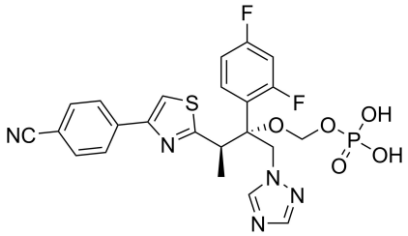

Figure 3: Fosravuconazole is the first and only drug currently in clinical trials against eumycetoma.

The financial weight and the isolation of the local communities, coupled with the debilitating nature of mycetoma mean this disease exacts a terrible burden on the affected communities. Recognition of mycetoma as a neglected tropical disease was the first step towards its eradication. Subsequently, in 2016, the Drugs for Neglected Diseases initiative (DND*i*), a non-governmental organisation that is another collaborator of the present project, in partnership with the pharmaceutical company Eisai, commenced a clinical trial of fosravuconazole against eumycetoma (**Figure 3**). Fosravuconazole has been found to be more effective against *M. mycetomatis in vitro* compared to itraconazole, but is less toxic than ketoconazole.[14] Yet there remains no other effective medicine to treat this disease, and there is little prospect of new medicines being developed because mycetoma lacks global awareness and financial investment, arising from a low expected return on that investment.

1.4. The Starting Point for Chemical Synthesis

To rectify the aforementioned shortfall, and given the high attrition rate of compounds that enter clinical trials, more drug candidates against eumycetoma need to be put forward alongside fosravuconazole. These new candidates could either serve as back-ups should the fosravuconazole clinical trial fail or work with fosravuconazole as a combination therapy, which would increase the effectiveness of treatment and minimise the development of drug resistance.

As a starting point in the search for new potential drug candidates, van de Sande screened 400 diverse drug-like compounds from the Pathogen Box, a free resource developed by the Medicines for Malaria Venture (MMV) and which has been used to kick-start new drug discovery projects.[15]

Of the 400 screened compounds, twelve were found to be potent against six isolates of *M. mycetomatis* (MIC = 0.007–8 μM) (**Figure 4**) (unpublished data). Although the middle row of **Figure 4** shows good minimum inhibitory

concentration (MIC) values, these compounds are privately owned and are not viable starting points for new projects in mycetoma. The fenarimol analogue MMV689244 (**Figure 4**, bottom row) is particularly interesting because this compound has a good MIC value and is from a public domain library under the name EPL-BS1246. This molecule was synthesised by the contract research organisation Epichem under contract from DND*i* for a drug discovery project relevant to Chagas disease. The library Epichem constructed for this project contains 700 fenarimol analogues for which extensive chemical and biochemical data has been obtained. These fenarimol analogues generally have low cytotoxicity (50–100 μM in L6 cells), moderate to good solubility (<1.6–100 μg/mL at pH 6.5) and moderate metabolic stability (<0.2–0.9 predicted ratio of hepatic extraction for human microsomes), all of which can be further optimised.[16] A promising initial effectiveness against mycetoma, the public domain status of the library and a wide range of modifiable analogues with favourable pharmacokinetic properties make the fenarimol series an attractive starting point for the present project.

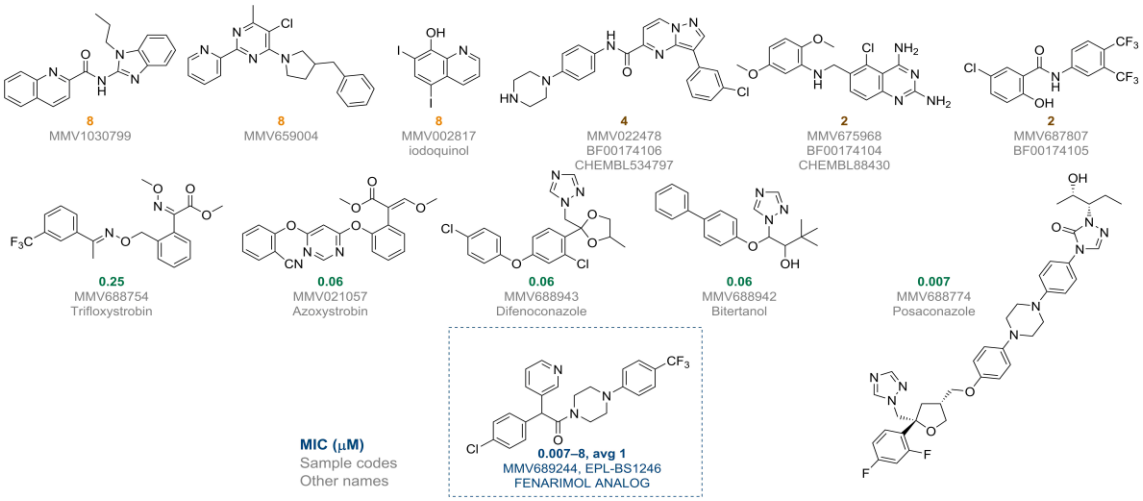

Figure 4: Twelve hits from the Pathogen Box highlights the fenarimol analogue as a promising starting point from the public domain.

In late 2016, van de Sande screened 35 compounds from the Epichem library (selected by DND*i* staff as being a representative subset with good associated metabolic and solubility parameters) and identified five potent hits against

isolates of *M. mycetomatis* (**Figure 5**, top row A) (unpublished data). The structures of the remaining 30 compounds were analysed (as part of the present project) and compiled into the general inactive motifs (**Figure 5**, middle row B). In general, the active compounds have either a triarylalcohol motif (i.e. three aromatic rings) or a diarylpiperazine motif (i.e. two aromatic rings with a piperazine ring). From these results, modifications to the five original hits were proposed by us (**Figure 5**, bottom row C) that would result in compounds not contained in the Epichem library and which could complement further screening of compounds from that library in the future. Modifications such as variations of aromatic substituents and conversion of aromatic to aliphatic rings would improve solubility. Modifications of hydrogen bond donors/acceptors and substitutions of piperazine rings could alter the way these molecules interact with their targets due to electronic and/or steric factors. Ring locks restrict bond rotation and can potentially change interaction of receptor drugs and their targets if such interaction requires a specific conformation. Results from the screening of the fenarimol analogues series in the Epichem library provides the foundation on which the present project is built.

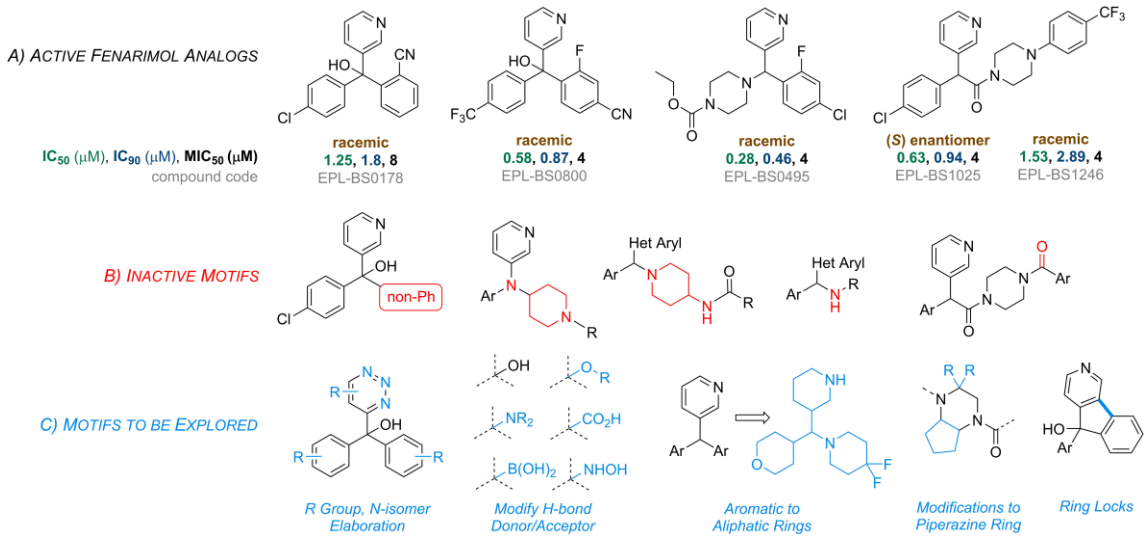

Figure 5: Results of the screening of fenarimol analogues in the Epichem library returned five promising hits against eumycetoma (top row A) and revealed some inactive motifs (middle row B). From these results, modified fenarimol analogues were proposed to improve potency (bottom row C).

1.5. Project Aims

Firstly, the original hits in the Epichem library (**Figure 5**, top row A) would be resynthesised to confirm their potency and the viability of the reaction pathway reported in the literature. Successfully resynthesised compounds would be biologically evaluated and compared to the original results using van der Sande's *in vitro* assay. EPL-BS1246 and its enantiopure counterpart EPL-BS1025 would be de-prioritised in the resynthesis phase because these two compounds currently serve as the back-up compounds for the DND*i* fosravuconazole clinical trial (**Chapter 1.3**) and exploration of this chemical space was considered redundant.

Secondly, modified fenarimol analogues would be synthesised and their biological evaluation results would guide further modifications of compounds in this series. Modifications would be chosen such that inactive motifs (**Figure 5**, middle row B) would be avoided. A small library of biologically evaluated modified fenarimol analogues would help elucidate chemical structures and properties of potent hits against eumycetoma and would be progressed to the *in vivo* model of the disease.

Thirdly, all operations in the present project would be carried out in accordance with open source principles whereby all data are made publicly available in essentially real time, contributions and suggestions are encouraged, and transparent collaborative efforts work towards a common goal without secrecy. A new social platform would be established to raise awareness for mycetoma and grant the general public access to research data to garner ideas and suggestions for directions of the project. By developing such a project structure, it was hoped that a community of scholars would eventually come together to accelerate research towards identifying new potential medicines for eumycetoma.

1.6. The Need for an Open Source Approach

The idea of "open source" originates from the sharing of source codes of a program to anyone who is interested, which resulted in novel platforms such as *Linux* and *Firefox*.[17] In the academic context, "open source" refers to the openness of ideas, discussions and data, as well as the recruitment of a larger audience both in the academic and general communities to achieve a common goal and the freedom of all participants to act as they please as equal partners.[18] Historically open source research has greatly powered the discovery process for antimalarial drugs and the antiparasitic drug praziquantel.[19-20] It is with high hope that by adopting a similar structure to Open Source Malaria, the present project would also accelerate drug discovery for mycetoma.

Neglected tropical diseases such as mycetoma often do not get research funding from major private investors like pharmaceutical companies due to the lack of financial return to recuperate large operational cost, which leads to no incentives to release proprietary knowledge.[21-22] However, once the intellectual and financial barriers (such as patents and profit) have been removed, there would be nothing holding back the speed of drug discovery but the limit of human and technological resources. Most importantly, the employment of an open source approach in the present project means progress made for the drug discovery of mycetoma would not result in individual gains (financial or otherwise) but rather benefit the patients of mycetoma whom need help the most (**Chapter 1.3**). On the other hand, these advantages must be weighed against the lack of a clear path to market for open source medicines because there has never been a public domain molecule arising from an open source project that has been taken all the way from discovery through trials to market. In the absence of such a precedent, other methods of financing drug discovery must be considered and these have recently been collected and summarised.[23]

1.7. Project Design

1.7.1. Choice of Chemical Space for Synthesis

In the present project, priority would be given to the resynthesis of potent initial hits against eumycetoma and that of structurally related compounds. The less active hits were expected to provide a general idea of undesirable motifs. However, the analysis and generalisation of the similarity between compounds in the Epichem library screening proved to be more challenging than expected because the screened compounds were specifically chosen for their chemical diversity. As such, it was difficult to tease out correlations between chemical structures and potency. Nonetheless, an attempt has been made and is presented in full in **Figure 6**, with **Figure 5** being a briefer, more generalised version.

The analysis revealed that only a few screened compounds have structures similar to the active compounds EPL-BS0178 and EPL-BS0800 (**Figure 6**, pink box). The promising potency exhibited by EPL-BS0800 meant that this limited triarylalcohol chemical space would be further explored in the present project as a first step.

More of the screened compounds had structures related to the active compound EPL-BS0495 (**Figure 6**, blue boxes). Since EPL-BS0495 has the best initial potency behind EPL-BS1246 and there were inexpensive commercially available reagents to readily modify the piperazine moiety, the diarylpiperazine chemical space was also selected to be further explored in the present project.

The majority of screened compounds are structurally similar to the most potent compound EPL-EPS1246 but have poor potency against eumycetoma (**Figure 6**, orange boxes). Based on this observation, and the status of EPL-EPS1246 as DND*i* clinical trial back-ups, exploration of this chemical space was considered redundant for the present project.

Proposed modified structures would be manually checked against the 700 compounds in the Epichem library. Interesting structures that are already present in this library would not be synthesised because samples of these compounds are being stored by DND*i* who can have them biologically evaluated against *M. mycetomatis.*

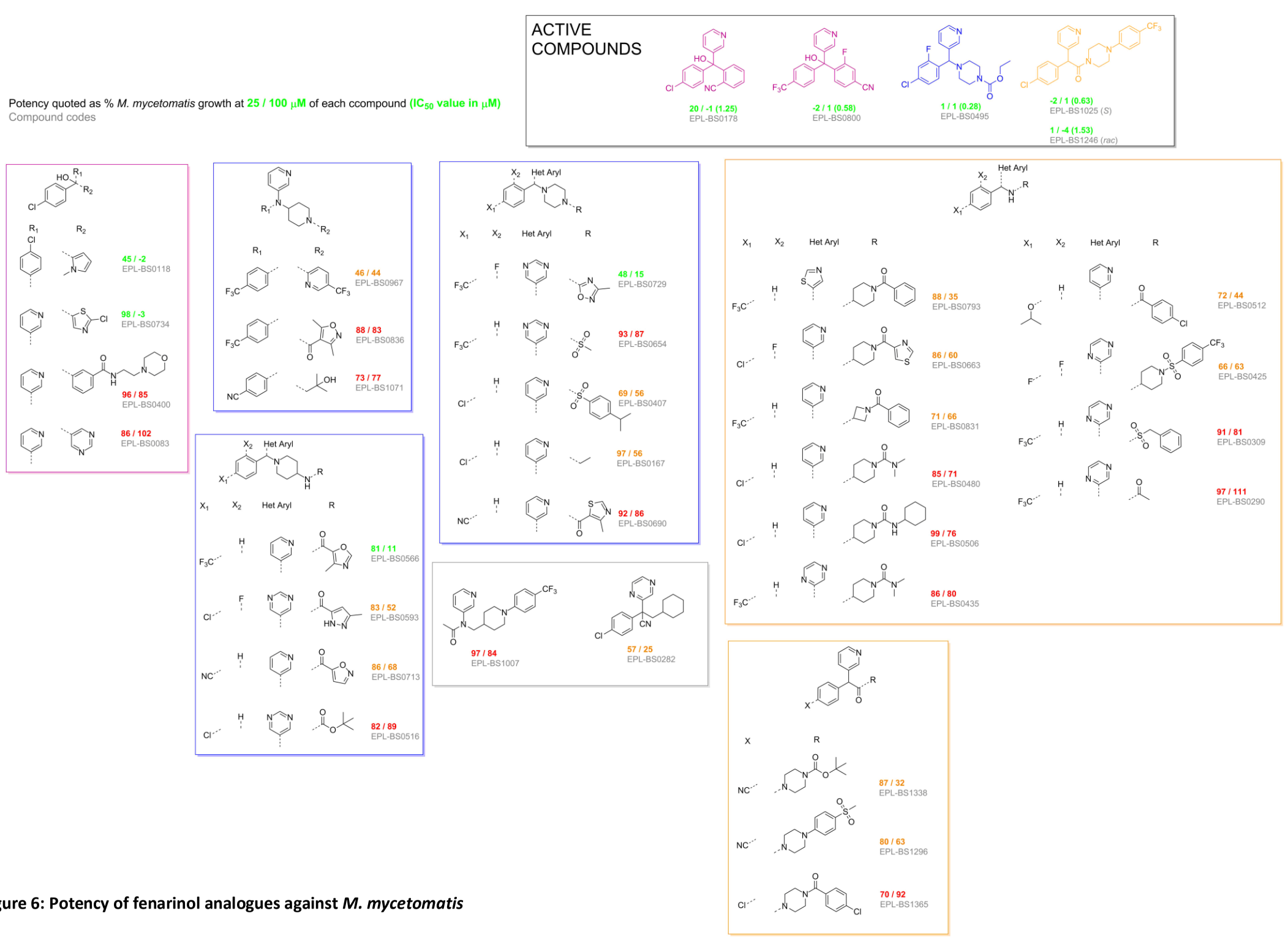

Figure 6: Potency of fenarinol analogues against *M. mycetomatis*

1.7.2. Project Timing

The creation of a community, and its infrastructure (see below) would begin in the present project, but it was decided to launch Open Source Mycetoma once the initial hits had been validated through resynthesis, to ensure that the wider community had an accurate and meaningful starting point with which to work. It was proposed that the data obtained, combined with follow-up *in vivo* evaluation of promising compounds, would constitute the dataset that launches the community project. Upon this launch the first request that would be made of the community would be an examination of the other compounds contained in the Epichem library to determine which would be most profitable to examine. Such evaluations would complement the synthesis of novel compounds arising from the present project and complement appeals that the project team may make to the wider academic and pharmaceutical community for any related, unpublished compounds that might be available for evaluation.

1.7.3. Open Source Methodology

The present project uses, as its core technology, the electronic lab notebook *LabArchives* which stores all primary research data and may be set to allow unrestricted (no log in) viewing in the public domain. The ELN for the present project can be accessed here: http://tinyurl.com/MyOS-HungELN

GitHub has been useful as a crowdsourcing (collaboration) platform for Open Source Malaria and would be used to host some public consultations in the future. In the present project, *Reddit* will be additionally used as a new social platform to raise awareness for mycetoma, generate discussions and gather suggestions from the general public. *Reddit* is the world's eighth most popular website and consists of many communities (termed *subreddits*) such as the Science *subreddit* (r/Science) which has over 17 million members making r/Science the fourth most popular community on *Reddit*. It is the popularity of these websites, particularly amongst young students, that makes them an attractive place to develop an active community of potential contributors.

To get started, a community for Open Source Mycetoma (r/OpenSourceMycetoma) was created. This site has a built-in Wiki function where general information about mycetoma can be displayed and also has a discussion function where research progress and questions can be posted (in both textual and pictorial formats) for comments and suggestions. Links to the *LabArchives* data can easily be provided to substantiate discussions. A cascading style sheet (CSS), which is a customisable coding functionality on *Reddit*, was implemented to make the user interface more attractive, intuitive and accessible. The site remains private until the (imminent) launch of the open source project, but can be seen in the screen shot below (**Figure 7**).

Any particular post on the *Reddit* community (**Figure 7**) may contain both images (red box) and/or texts in the form of a "stickied comment" (yellow box) to inform users with relevant data or requests for actions. Users can then choose to provide their inputs by commenting on the same post (yellow box) or creating a new post (yellow arrow). The sidebar (black box) serves as a dashboard which gives an overview of the site's objectives. Hyperlinks enable redirection of users to places of interest within the community (black arrow) such as the Wiki page for mycetoma or to external sites such as *LabArchives* (red arrow). Users may "upvote" or "downvote" a post or comment to increase the exposure of high quality contents and deprioritise poor quality or irrelevant contents. Moderation (both manual and automatic) provides an extra layer of protection against undesirable contents. CSS provides the overall professional yet attractive look to the page and scientific concepts is explained to the public audience using plain English.

The use of *LabArchives*, *Reddit* and other social media platforms (such as *FaceBook* and *Twitter*) will turn the present project into a truly open source project and help give mycetoma the attention needed from the wider scientific community to fast track drug discovery, even though these sources are unorthodox at first glance from an academic point of view.

With these components ready for deployment, attention turned to the core focus of the project, which was the validation of the initial hits, the synthesis of new

analogues and the evaluation of these compounds in both in vitro and in vivo assays of eumycetoma.

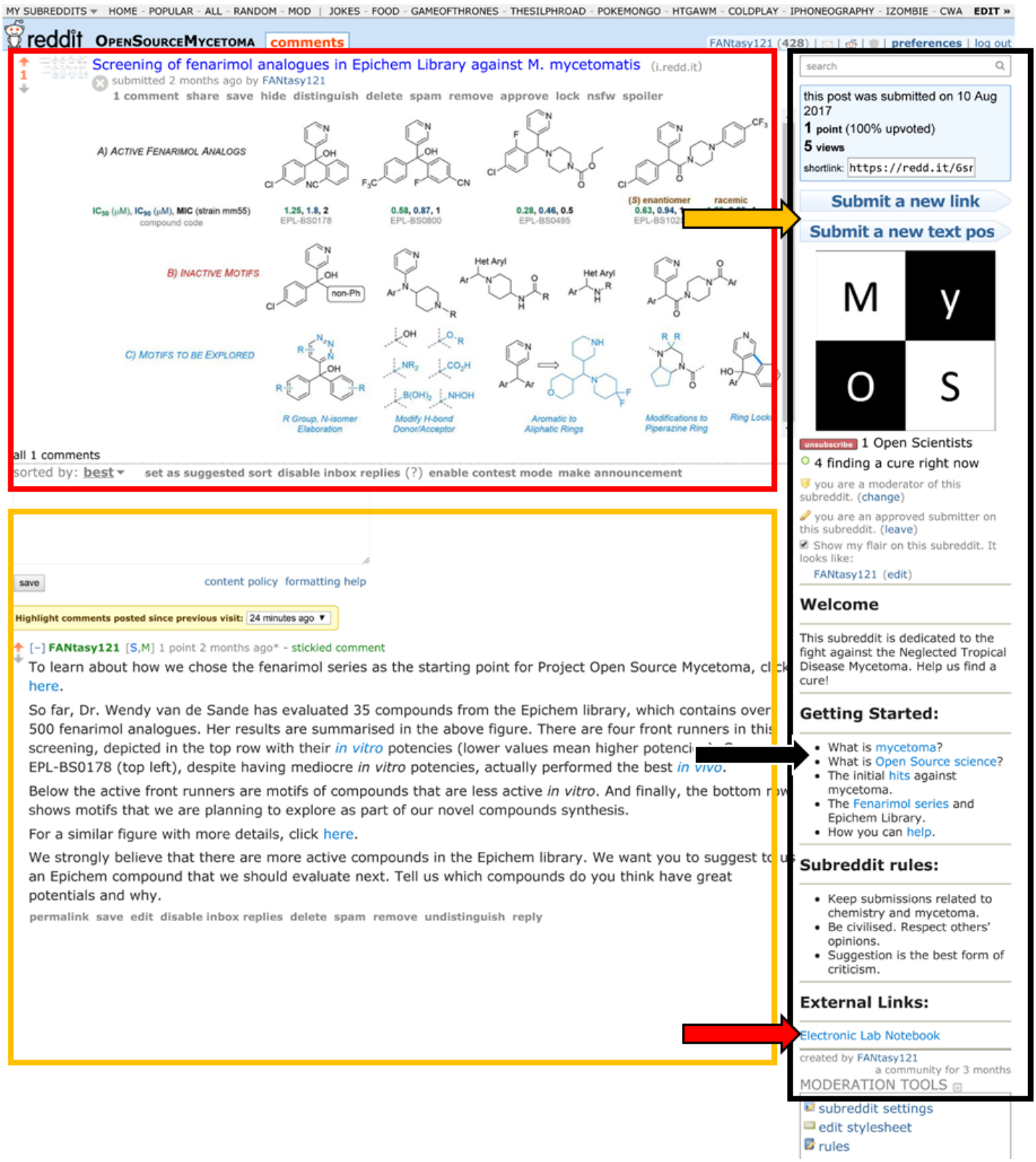

Figure 7: A sample page of the Open Source Mycetoma Community.

Chapter 2: Results and Discussion

2.1. Synthesis of EPL-BS0800 and Novel Analogue

2.1.1. Synthesis of EPL-BS0800

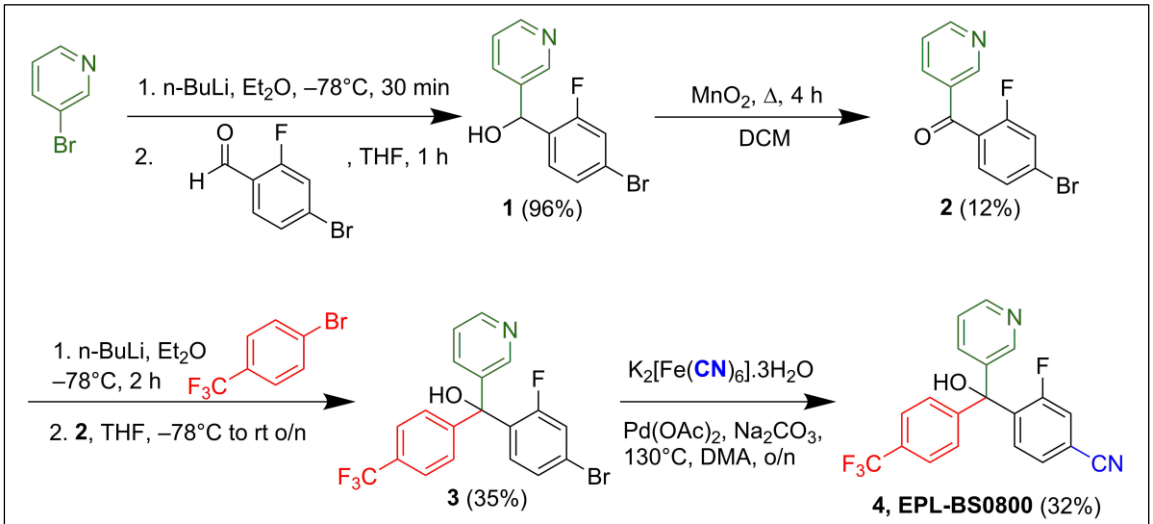

Scheme 1 Synthetic pathway for EPL-BS0800

The synthesis of EPL-BS0800 was successfully carried out with procedures based on a literature report (**Scheme 1**).[16] Although spectroscopic characterisation was scant for the final product and its precursors, the reactions were well described.[24-26]

3-Bromopyridine (**Scheme 1**, green) was lithiated with *n*-butyllithium, the molarity of which was established with a literature titration method,[27] before being used for a nucleophilic attack on the carbonyl carbon of the aldehyde, which afforded diarylalcohol **1** upon workup. The *n*-butyllithium was only equimolar to the bromopyridine and the reaction was well mixed before the aldehyde was added, which ensured the thorough lithiation of the bromopyridine to reduce the unwanted side reaction (cross-lithiation) with the

bromide on the aldehyde. Ethereal solvents such as diethyl ether and THF enhance the reactivity of the organolithium reagent by preventing oligomeric aggregation and polarising the carbon-lithium bond due to non-bonding interactions of lone pairs on the oxygen with the lithium.[28-29] However, because the organolithium is a strong base (pKa ~ 50), it can also abstract hydrogen atoms from water and acidic hydrogens adjacent to the oxygen in solvent molecules.[30-31] To prevent this undesirable interaction, the reaction was carried out under a dried inert environment at −78°C. These precautions ensured a high yield of 96% in the first step of the resynthesis.

The diarylalcohol **1** was oxidised to ketone **2** using activated manganese dioxide. Experimentation of this reaction showed that the particle size of manganese dioxide was important for successful catalysis. When non-activated manganese dioxide (particle size >10 μm) was used, no conversion occurred (as judged by TLC analysis of the crude reaction mixture and confirmed by ^{1}H NMR). When activated manganese dioxide (particle size <10 μm) was used (3 equivalents), the reaction yielded **2** (12%) and recovered **1** (50%) which was lower than expected (78% reported in literature).[16] Due to erroneous interpretation of the TLC result for this reaction arising from the discrepancy in intensities between the alcohol and ketone spots on the TLC plate under UV light, the reaction was prematurely terminated. For future iterations of this oxidation reaction, more equivalents of manganese dioxide could be added to ensure higher conversion, but enough material was secured from this reaction to allow the synthesis to proceed.

Similar to the organolithium reaction with bromopyridine (**Scheme 1**, green), the aryl bromide (**Scheme 1**, red) was lithiated with *n*-butyllithium before ketone **2** was introduced for nucleophilic attack. The reagent stoichiometry and solvent choice remained the same as for the first step of the synthesis. The yield of triarylalcohol **3** was lower than that of diarylalcohol **1** because the carbonyl carbon in **2** is more sterically crowded. However, the experimental yield (35%) was lower than the reported value (70%)[16] possibly due to the employment of an older supply of *n*-butyllithium that was not titrated prior to use. The product generated was necessarily racemic because the nucleophilic organolithium

reagent could attack from either face of the carbonyl carbon in **2**. Such synthetic steps in this project were carried out in awareness that, should biological evaluation result in a potent hit, then resolution, e.g. *via* chiral column chromatography, could be employed to examine whether one enantiomer is more biologically active than the other (*i.e.*, determination of the so-called *eudysmic ratio*).

Aryl bromide **3** was coupled with the cyanide from potassium hexacyanoferrate using palladium acetate as the catalyst to give benzonitrile **4**. This reaction highlights the use of metal catalysis without an added ligand. Sodium carbonate is thought to speed up the reaction by acting as a Lewis base and reducing inactive Pd(II) to active Pd(0).[26] Furthermore, as a cyanating reagent, potassium hexacyanoferrate is non-toxic because the strong iron-cyanide bond does not readily dissociate into toxic cyanide when taken up into the body. In fact, potassium hexacyanoferrate is used as an anti-caking agent in table salt.[32] In comparison, according to material safety data sheets, traditional cyanide sources like sodium/potassium/copper cyanide are all fatal by skin contact, inhalation or ingestion. Dimethylacetamide was chosen because it is a high-boiling solvent resistant to decomposition, which facilitates the temperature required for this milder type of cyanation.[26]

The literature source did not propose a mechanism for this cyanation reaction but suggested that it might proceed *via* a pathway similar to Heck, Suzuki and Sonogashira reactions.[26] The benzonitrile **4** was obtained in slightly higher yield than expected (32% *c.f.* 27% from literature).[16] There are instances in the literature source where this cyanation stalled well before complete conversion when a challenging substrate was used and aryl bromide **3** might be one such substrate.[26] The ease of handling this reaction due to its low toxicity outweighs its limitation of giving a modest yield. Moreover, this cyanation is reported to tolerate a range of functional groups including alcohol, ketone and aldehyde so the synthetic route to benzonitrile **4** could be further optimised by introducing the cyanation step earlier in the synthetic scheme.[26] In the present project, the cyanation was the final step because aryl bromide **3** was also an interesting

candidate for biological evaluation, to test whether the cyanation was actually required for potency.

2.1.2. Synthesis of Novel EPL-BS0800 Analogue

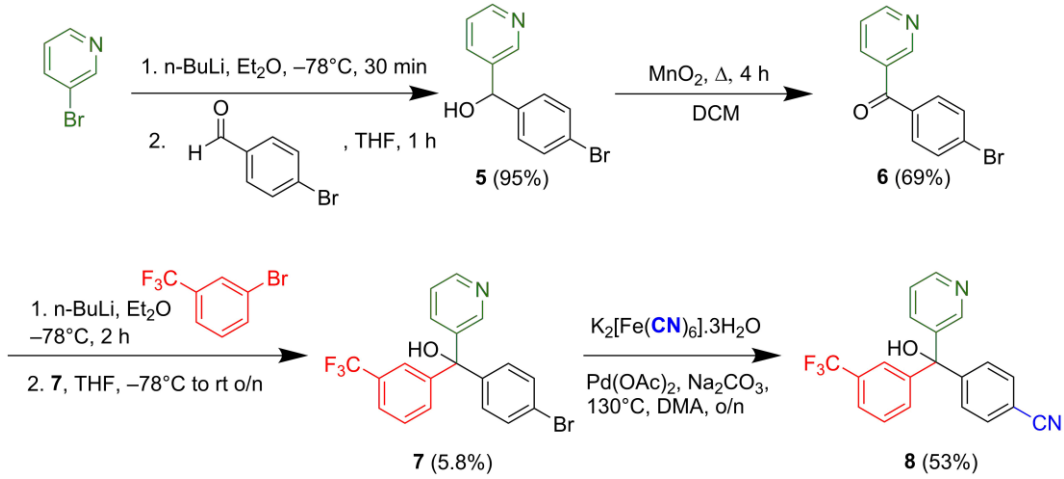

Scheme 2: Synthetic route to EPL-BS0800 analogue

The synthetic route of EPL-BS0800 was adapted to a modified analogue **8** in which the trifluoromethyl group is in the *meta* (rather than *para*) position and the aromatic fluoride group was replaced with a hydrogen atom (**Scheme 2**). Alcohol **5** was oxidised to ketone **6** with extra manganese dioxide (5 equivalents, *vs.* 3 equivalents for **2** in **Scheme 1**), which significantly increased the yield (68% of **6** *vs.* 12% of **2**). When freshly titrated *n*-butyllithium was used for the organolithium reaction with **6**, triarylalcohol **7** was still obtained in poor yield, eliminating the possibility of *n*-butyllithium concentration being the culprit for this yield, as previously suspected. The longer reaction time employed was the other factor that could have impacted on the yield of **7** because the reactive organolithium might have formed degradation products with the solvents owing to its strong basicity,[30-31] evident by the formation of intractable side products (27% of the crude yield). It was proposed that a reduction in reaction time would greatly improve the yield of this reaction. Nevertheless, sufficient yield of **7** was obtained for cyanation to afford the EPL-BS0800 analogue **8**.

At the time of completion of the above synthetic route, the *in vivo* assay results showed that EPL-BS0800 exhibited the worst potency of all five original hits in the larval model (see **Chapter 2.4.2**, **Figure 12**). In keeping with the aims for the present project, one of which was to let biological evaluation results guide synthesis of novel analogues (**Chapter 1.5**), further exploration of EPL-BS0800 analogues was put on hold. EPL-BS0178 exhibited the best *in vivo* potency despite having the worst *in vitro* result so resynthesis of this compound and exploration of its analogues became a higher priority. The discrepancy between *in vitro* and *in vivo* potencies accentuates the challenge in drug discovery for eumycetoma due to the exclusive grain formation in the *in vivo* model (**Chapter 1.2**).[33]

2.2. Synthesis of EPL-BS0178 and Novel Analogues

2.2.1. Resynthesis of EPL-BS0178

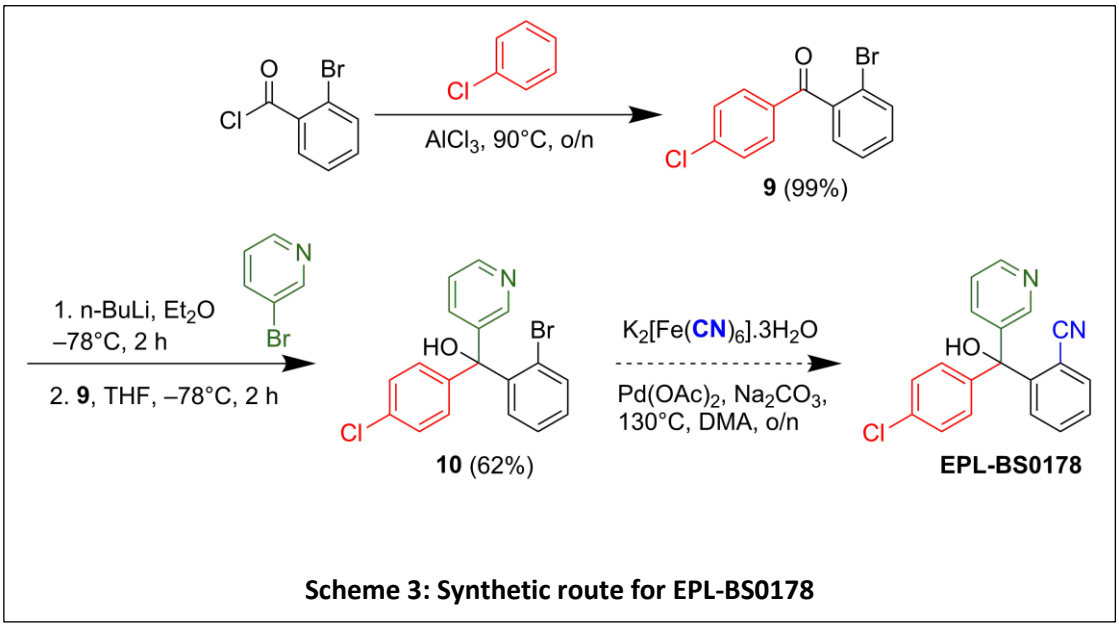

Scheme 3: Synthetic route for EPL-BS0178

Friedel-Crafts acylation of 2-bromobenzoyl chloride with chlorobenzene afforded ketone **9** (**Scheme 3**).[16, 34] Chlorobenzene was used both as the solvent and the nucleophilic reactant. Aluminium trichloride is thought to abstract a chloride ion from 2-bromobenzoyl chloride to form aluminium tetrachloride

anion and bromobenzoyl acylium cation (**Scheme 4**, E+), the latter of which is attacked by chlorobenzene's π electrons. The chloro- substituent is an *ortho/para* director because chloride can delocalise its lone pairs of electrons to stabilise the non-aromatic carbocation intermediate, which re-aromatises upon deprotonation to give ketone **9**.[35-36] Only the *para* acylated product was observed in this reaction, possibly because nucleophilic attack is sterically more hindered at the *ortho* position. This regioselectivity was confirmed by the relevant coupling patterns being observed in the ^{1}H NMR spectrum of the product and the result was consistent with those reported in the literature.[16, 34]

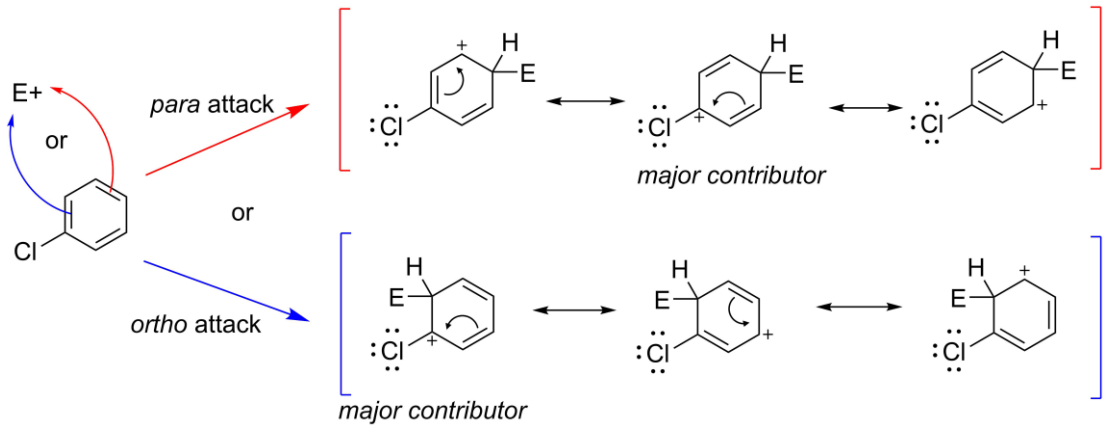

Scheme 4: Resonance structures of the Friedel-Crafts intermediates

Similar to previous organolithium reactions in the synthesis of EPL-BS0800 (**Scheme 1**), the bromopyridine (**Scheme 3**, green) was lithiated with *n*-butyllithium before ketone **9** was introduced for nucleophilic attack. The shortened reaction time compared to previous organolithium reaction attempts (2 hours in **Scheme 3** *vs.* overnight in **Scheme 1** and **Scheme 2**) greatly increased the yield of triarylalcohol **10** (62%) compared to previous attempts. The recovery of ketone **9** (12%) and the lack of any other major side products (unlike previous reactions) suggest that the reaction time could be slightly extended to further improve the yield.

Cyanation of aryl bromide **10** using the same method for the synthesis of benzonitriles **4** and **8** gave no conversion to EPL-BS0178. Doubling of either the reaction time or the equivalents of potassium hexacyanoferrate and palladium

acetate gave no benzonitrile conversion. Re-evaluation of the cyanation method reported by Keenan *et al.* (2012)[16] showed that the original method, reported by Weissman *et al.* (2005),[26] used a different ratio of reagents. For the Keenan method, an excess of potassium hexacyanoferrate and DMA solvent could result in more dissolved cyanide ions which would react with the catalyst to form the inactive palladium cyano species.[26] When the reaction conditions were adjusted to the method reported by Wiessman *et al.* again no conversion was observed, however. Given that cyanation was successful for benzonitriles **4** and **8** where the bromide is in the *para* position and there was no literature report for cyanation of **10**, *ortho* bromide cyanation might not be successful due to steric hindrance. This theory could be tested in future by cyanation of ketone **9** before the organolithium reaction stage.

At this stage in the project, *in vitro* assays showed that benzonitriles **4** and **8** were only slightly more potent than their respective aryl bromides **3** and **7.** Due to time constraints, optimisation of **Scheme 3** to obtain EPL-BS0178 was not attempted. Instead it was thought to be a better strategy to pursue more significant variations in structure from aryl bromide **10** towards EPL-BS0178 analogues.

2.2.2. Synthesis of Novel EPL-BS0178 Analogues

Using triarylalcohol **10** as a starting point, a Williamson ether synthesis afforded triarylether **11** (**Scheme 5**, top).[37] This compound is of obvious strategic importance in evaluating whether the central OH group is required for biological activity. Deprotonation of the alcohol by sodium hydride forms an alkoxide which activates **10** for nucleophilic attack with added methyl iodide. Since the Williamson reaction proceeds *via* an S_N2 mechanism,[38] methyl iodide is the ideal alkylating agent because it has a good leaving group and is not sterically hindered (this also determined the choice of making the *methyl* ether analogue). However, because the alkoxide generated from **10** is bulky, the reaction rate was expected to be slow so the reaction time was extended overnight. The polar aprotic solvent THF was a good solvent choice for this reaction because THF has no labile proton to compete with the triarylalcohol for deprotonation or to H-

bond with the subsequent alkoxide which would reduce the alkoxide's nucleophilicity.[39] Overall the ether analogue **11** was obtained in 33% yield.

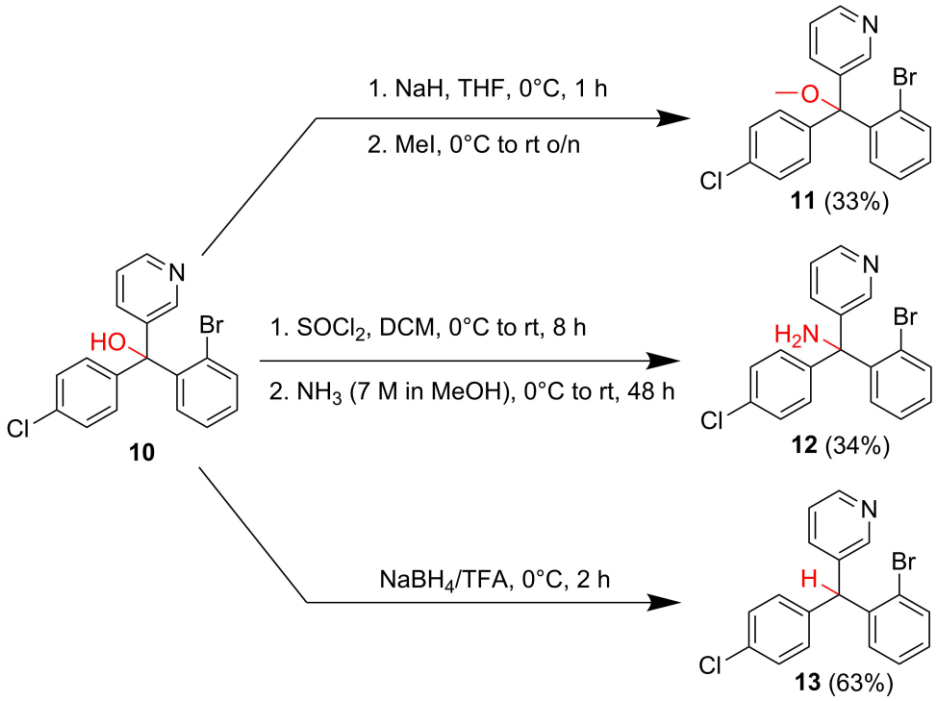

Scheme 5: Synthetic routes for EPL-BS0178 analogues

Tertiary amine **12** was formed by the activation of triarylalcohol **10** with thionyl chloride followed by amine substitution (**Scheme 5**, middle). The substitution reaction involved in the synthesis of **12** is likely to proceed *via* an S_N1 mechanism because, upon thionyl chloride converting the alcohol in **10** (a bad leaving group, pKa ~ 15) into an aryl chloride (with a much better leaving group, pKa ~ –6), the carbocation generated from **10** can be stabilised by partial electron delocalisation from the three neighbouring aromatic rings, with polar solvents like DCM and methanol further stabilising the carbocation.[40-41] Nucleophilic addition of ammonia would then give amine **12**. The reaction was performed at 0°C to control the exothermic reaction with thionyl chloride and limit undesirable side reactions caused by primary amine **12**. This reaction afforded a better yield of the amine than expected (34% *vs.* 24% for a similar substrate) because the literature method did not activate the alcohol before nucleophilic attack.[16] A higher concentration of ammonia would be expected to

improve the yield for this reaction in the future.[16, 37] This compound is of value for biological evaluation since it introduces a different H-bond donor while opening up the possibility of further novel divergent functionalisation of the amine at a later stage in the project.

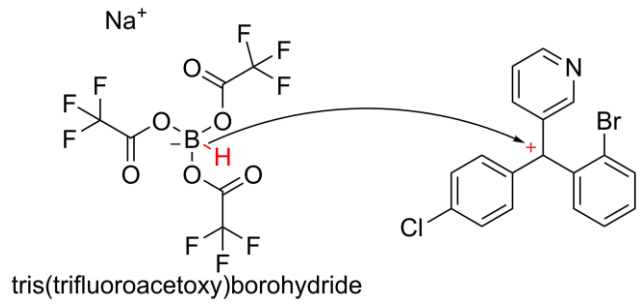

Scheme 6: Nucleophilic attack of a hydride reducing reagent with a tertiary carbocation

Reduction of triarylalcohol **10** using sodium borohydride/TFA afforded triarylmethane **13**.[42] TFA protonates the alcohol in **10** making -OH a good leaving group which would, upon leaving, generate a stabilised tertiary carbocation (**Scheme 6**, right).[43] At the same time, the addition of sodium borohydride into TFA also generates the tris(trifluoroacetoxy)borohydride species *in situ* which acts as a hydride source and attacks the carbocation to form **13** (**Scheme 6**).[43] This reaction was expected to be milder than the traditional hydride reducing reactions and produce moderately high yields for tertiary alcohol, which was reflected in the yield of **13** (63%).[42] This compound was synthesised to assess whether any polar group is required in the -OH position at all for biological actvity.

With the novel EPL-BS0178 analogues in hand, ready for biological evaluation, attention was turned to the synthesis of EPL-BS0495 and its novel analogues.

2.3. Synthesis of EPL-BS0495 and Novel Analogues

2.3.1. Resynthesis of EPL-BS0495

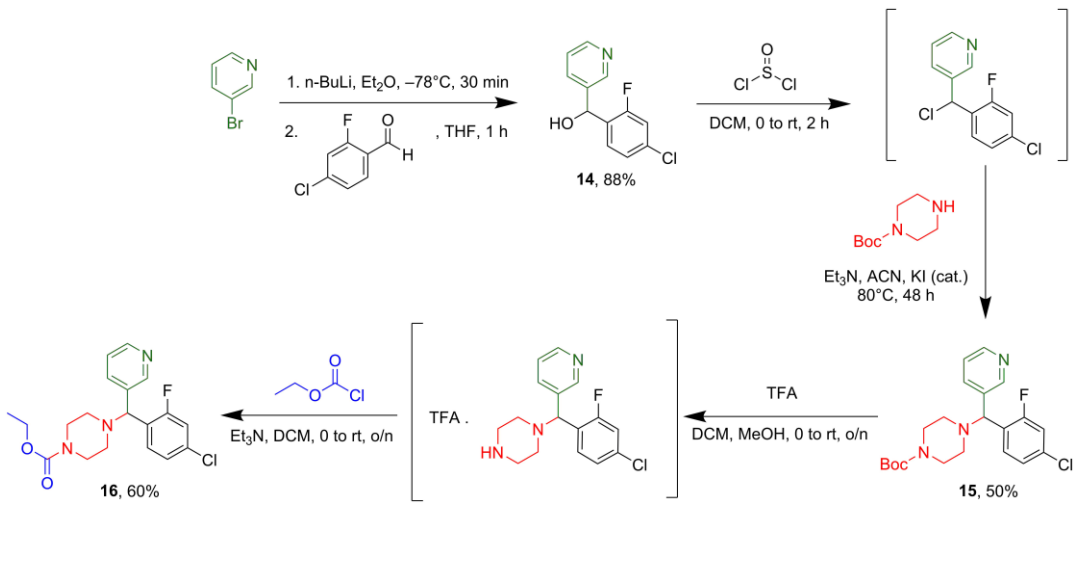

Scheme 7: Synthetic Route for EPL-BS0495

The synthesis of EPL-BS0800 was successfully carried out with procedures based on a literature report (**Scheme 7**).[44] Lithiation of bromopyridine (green) generated the organolithium reagent that was used for the nucleophilic attack on the benzaldehyde (black) to afford **14** (88%). This reaction continued to be a robust, straight forward and high yielding route to form diarylalcohols as was expected from previous attempts to form **1** (96%) and **5** (95%).

In a similar manner to triarylamine **12** (**Scheme 5**, middle), diarylpiperazine **15** was synthesised by using Boc-piperazine (**Scheme 7**, red) for the nucleophilic attack of the aryl chloride intermediate which was activated from alcohol **10** using thionyl chloride. The yield (50% over two steps) was lower than expected (literature 72% over two steps[44]) the reaction mixture of the aryl chloride intermediate reacted more violently than expected with the quenching reagent even when the quenching reagent was cautiously added portionwise. For future iterations of this reaction type (described below), quenching took place in an ice bath with the quenching reagent added even more slowly.

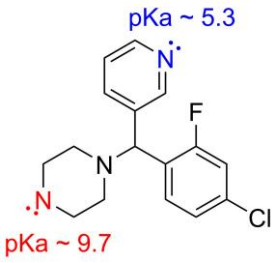

Figure 8: pKa values of piperazine and pyridine.[45-46]

Deprotection of the Boc group in **15** with TFA gave the TFA salt intermediate that, when basified and used as a nucleophile to attack ethyl chloroformate (**Scheme 7**, blue), afforded EPL-BS0495 (60%) on a gram scale. The simplicity and scale of this process demonstrates the overall robustness of this synthetic route. Ethyl chloroformate was used in slightly less than 1 equivalent *vs.* the piperazine nucleophile to prevent the undesirable second acylation of the less nucleophilic pyridinyl nitrogen (**Figure 8**, blue). Synthesis of EPL-BS0495 could be optimised *via* a convergent pathway in which the Boc-piperazine (**Scheme 7**, red) was acylated with the chloroformate (**Scheme 7**, blue) before being deprotected and coupled with the aryl chloride intermediate. In the present project, linear synthesis was favoured because diarylpiperazine **12** was an attractive diversification point for coupling with various chloroformates (see **Section 2.3.2.1**).

2.3.2. Synthesis of Novel EPL-BS0495 Analogues

2.3.2.1. Modification of the Carbamate Moiety

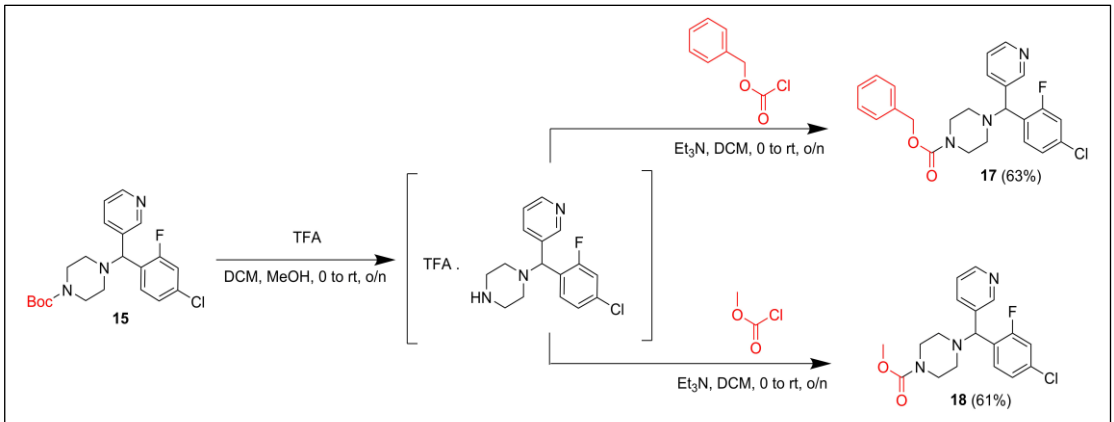

Scheme 8: Synthetic routes for carbamate variation of EPL-BS0495 analogues

The TFA salt of deprotected **15** was used (again, following basification) for nucleophilic attack on benzyl chloroformate (top) and methyl chloroformate (bottom) to afford two novel carbamate variations **17** (63%) and **18** (61%) (**Scheme 8**), using the same method previously described in the EPL-BS0495

resynthesis. Interestingly, the bulkiness of the chloroformates did not appear to hinder the nucleophilic substitution of the TFA salt intermediate as **16**, **17** and **18** were obtained in comparable yields (~60%). These compounds are important for the understanding of any quantitative structure-activity relationship since they will probe whether non-polar interactions in this region may be important for activity, or indeed whether the carbamate pendant as any influence on the activity or may, instead, be fragmented *in vivo*.

2.3.2.2. Modification of the Piperazine Moiety

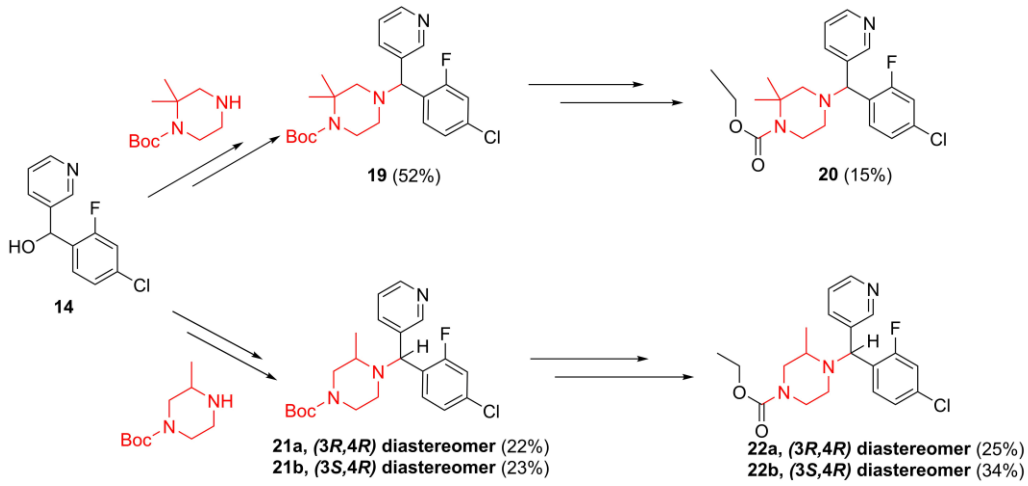

Scheme 9: Synthetic routes for piperazine variation of EPL-BS0495 analogues.

Novel substituted piperazines **20** and **22** were synthesised according to the method described in the resynthesis of EPL-BS0495, with the relevant commercially-available Boc-piperazines being used as starting materials (**Scheme 9**, red). The yield of **19** (52%) was similar to previous attempts of this reaction. The methyl group on Boc-methylpiperazine could have caused steric hindrance during nucleophilic attack, which would cause a slight reduction in the yield (**21,** 45% total). Similarly, the bulkier dimethyl substituents on **19** presented a steric challenge for the acylation step, drastically reducing the yield of **20** (15%).

The monomethyl-substituted piperazine reagent was racemic, meaning **21** was formed as a mixture of diastereomers. These could be separated by column chromatography (**21a** and **21b**, formed in essentially identical yield) and were

separately deprotected and acylated to afford diastereomeric products **22a** and **22b**. Both reactions for this final step gave poor yields because of the reaction scale was small and the difficulty of handling the reactive, volatile ethyl chloroformate (on 10 μL scales) probably lowered the stoichiometry of the acylating reagent. Ethyl chloroformate was used in restricted equivalents to prevent unwanted side reactions as outlined earlier. For future iterations of this reaction, more equivalents of ethyl chloroformate could be used to address the volatility problem but care must be taken to strike a balance between ensuring optimal yields and avoiding the unwanted diacylated products.

The yields of **21a** and **21b** did not allow for recrystallisation to obtain X-ray crystallographic data and assign relative stereochemistry. Instead, a computational study was performed to rationalise the structural variations between the two isomers which would explain the differences in ^{1}H NMR spectroscopic shifts of these isomers. The structures of different parts of the diaryl-Boc-piperazine **21** were simplified and optimised using approximation of the Schrödinger equation $\hat{H}\Psi = E\Psi$.[47] By solving for the energy E, the minimum energy (optimised) structures would be realised.[47] The Hamilton operator $\hat{H}$ was approximated with the Restricted Hartree-Fock level of theory where electron correlation was ignored (electrons do not repel each other) and electrons fill molecular orbitals in opposite spins.[48] The Born-Oppenheimer approximation was invoked where electrons travel infinitely faster than nuclei such that their motions can be treated separately to calculate the electronic and nuclear components of the wavefunction ($\Psi_{total} = \Psi_{nuclear} \times \Psi_{electronic}$).[49] The electronic wavefunction $\Psi_{electronic}$ was then approximated with the 6-31+G(d) basis set where 6 Gaussians was used to model the core orbitals, 3 Gaussians were used to model the valence orbitals and 1 extra Guassian allowed for flexibility of modelling. Polarisation functions were added to model the orbital contraction that occurs when bonds are formed and diffuse orbitals were added to allow for the orbital expansion of electronegative atoms which are present in the structure of **21**.[50] Although these simplification and approximations appear to be extreme, they are necessary to reduce to high computational cost that modelling for the complexity of **21** would no doubt entail. These minimisations are used as an

approximation to the conformations of the molecule in solution that might give rise to the observed signals.

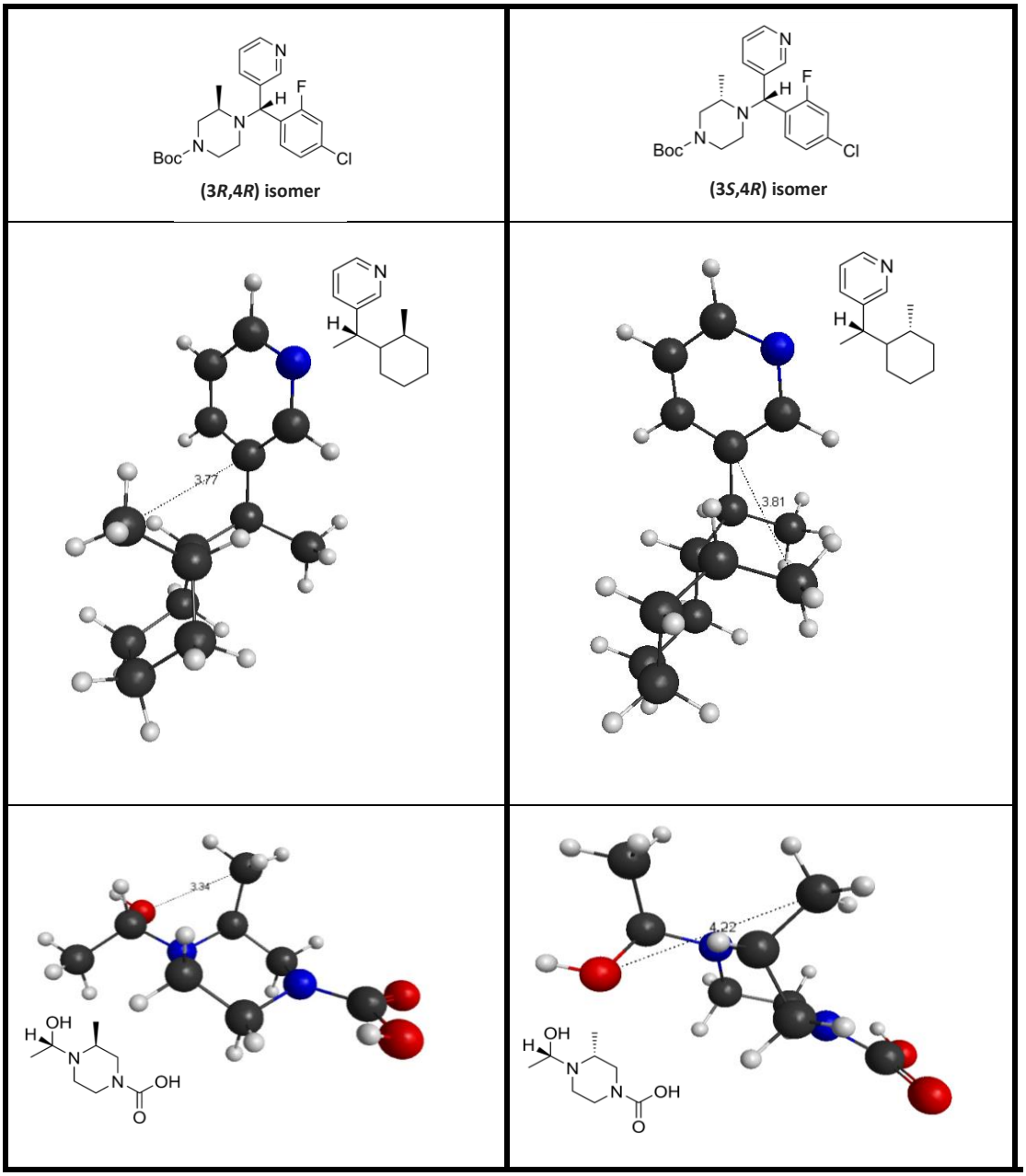

Figure 9: RHF/6-31G+ optimised structures of models for the (3*R*,4*R*) isomer (left column) and the (3*S*,4*R*) isomer (right column). (Black=C, white=H, blue=N, red=O; distance (dashed lines) is in Å.

The optimised structures of the simplified models for isomers of **21** are shown in **Figure 9**. The (3*R*,4*R*) and (3*S*,4*R*) isomers were used for the analysis. When the benzene ring was omitted and the piperazine ring was approximated with a cyclohexane (**Figure 9**, middle row), the optimised structures show that the piperazine methyl group of the (3*R*,4*R*) isomer directly faces the pyridine ring whereas, for the (3*S*,4*R*) isomer, the same methyl group faces away from the pyridine ring. When the pyridine group was approximated with an alcohol and the Boc-group was approximated with a carboxylic acid (**Figure 9**, bottom row), the (3*S*,4*R*) isomer methyl group also faces away from the alcohol while the (3*R*,4*R*) isomer methyl group does not. Proximity to an aromatic ring would enable H-π interaction and also expose the methyl group to the deshielding magnetic field generated by the aromatic ring current.[51] Thus the (3*R*,4*R*) isomer was expected to have its methyl ^{1}H NMR peak shifted downfield compared to that of the (3*S*,4*R*) isomer.

MestReNova prediction of the ^{1}H NMR spectra for the two isomers provided evidence for the methyl peak being shifted more downfield for the (3*R*,4*R*) isomer compared to the (3*S*,4*R*) isomer (**Figure 10**, top, red oval).[52] Furthermore, the predicted spectra also showed the peak for the proton stereocentre of the (3*R*,4*R*) isomer being shifted downfield (**Figure 10**, top, yellow circle) and the protons adjacent to the pyridine nitrogen being slightly shifted downfield (**Figure 10**, green box). Comparison of these features with the experimental spectra of the two isomers gave good agreement with these predictions and hence the assignment that **21a** was the (3*R*,4*R*) isomer and **21b** was the (3*S*,4*R*) isomer (**Figure 10**, bottom, circled). Acylation of **21a** and **21b** retained these spectroscopic features in **22a** and **22b**. Differences in chemical shifts of ^{13}C NMR spectra were also observed but, due to time constraints, were not additionally rationalised in detail.

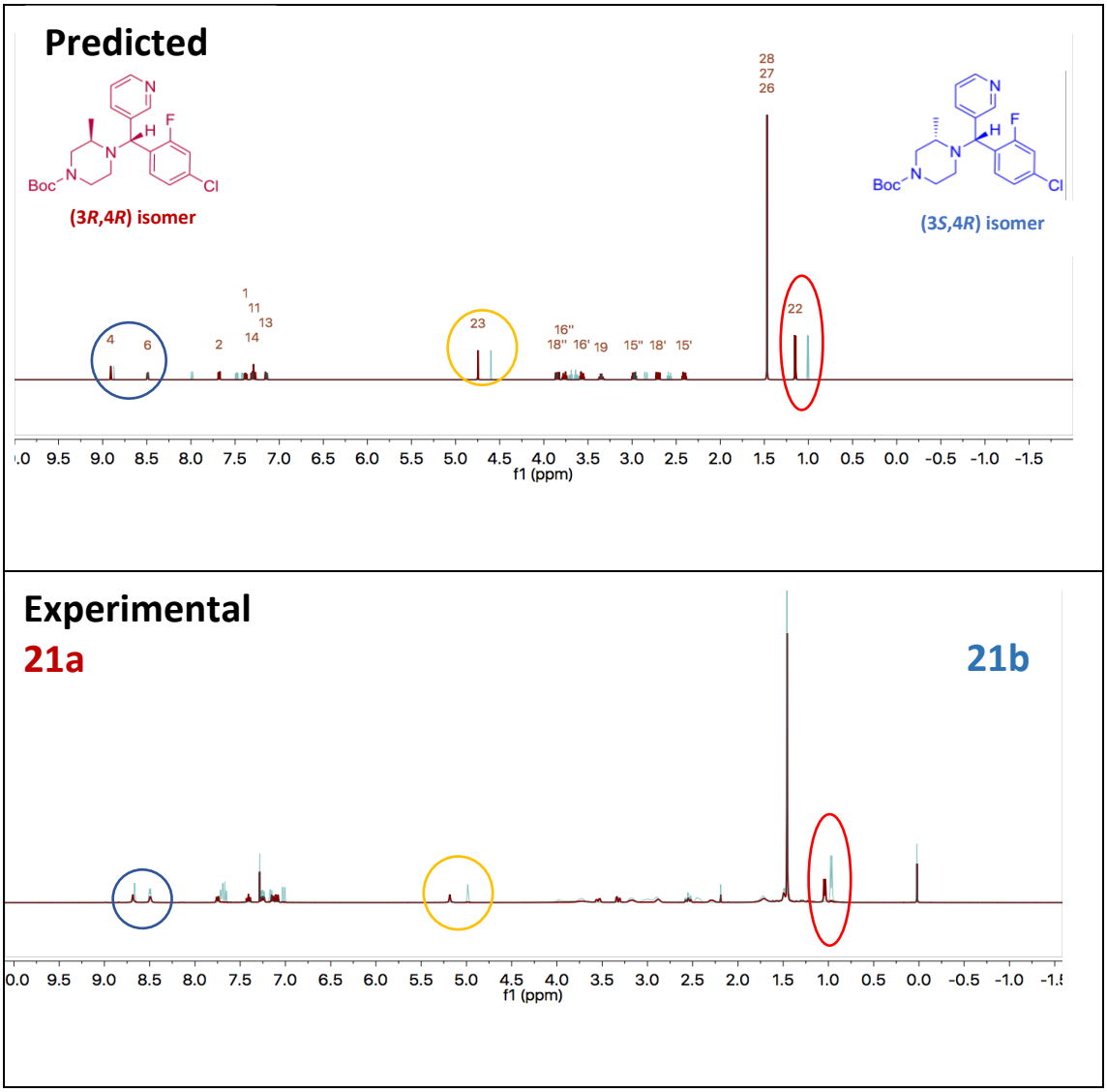

Figure 10: (Top) Superimposed predicted 1H NMR spectra for the *(R)-(R)*-isomer (maroon) and *(S)-(R)*-isomer (blue). (Bottom) Superimposed experimental 1H NMR spectra for *21a* (maroon) and *21b* (blue).

At this point, a small library of resynthesised and novel compounds had been generated. The synthesis phase of the present project was complete. Resynthesised and novel compounds were sent for biological evaluation (see **Figure 11** for more details). A combination of these data with existing data on related compounds would start to provide an understanding of desirable features of small molecules for bioactivity against eumycetoma.

2.4. Biological Evaluation

2.4.1. *In Vitro* Efficacy

To assess the *in vitro* potency of candidate compounds, suspensions of a model strain of *M. mycetomatis* were mixed with various concentrations of the fenarimol analogues. After incubation, these suspensions were measured spectrophotometrically to examine the growth inhibition, which was plotted against the concentrations to determine IC_{50} and IC_{90} values (see Experimental Section for more information). Besides the most common strain (m55), seven other strains of *M. mycetomatis* were tested to determine the minimum inhibitory concentrations. The *in vitro* results for fenarimol analogues synthesised in the present project are summarised in **Figure 11**. The raw data used to create these plots were generated by Dr. Wendy van de Sande (Erasmus MC University, Rotterdam) and used with permission.

The resynthesised compounds **4** and **16** both exhibited higher potency (MIC50 = 1 and 0.5 μM) compared to the corresponding initial samples of EPL-BS0800 and EPL-BS0495 respectively (MIC's = 4 μM) (**Figure 11**). This discrepancy could have resulted partial decomposition during the long-term storage of these compounds in DMSO after they were synthesised as drug candidates for another disease; clearly **4** and **6** were freshly synthesised in the present project this year and were assayed shortly after synthesis.

The change of a bromo- substituent to a nitrile- substituent (**3** *vs.* **4** and **7** *vs.* **8**) saw only a marginal increase in the *in vitro* effectiveness, which suggests that the nitrile substituent is not the primary reason for potency (**Figure 11**) and is perhaps unnecessary. The changes effected in the carbamate group do not appear to impact seriously on potency (**Figure 11**, **15** *vs.* **16**). It is possible that the carbamate is labile under the conditions of the assay and that these compounds could ultimately act as prodrugs. Interestingly, compounds lacking the fluoro- substituent exhibit drastically diminished potency compared to similar compounds which have the fluoro- substituent (**Figure 11**, **3** *vs.* **7**; **4** *vs.* **8**; **15** and **16** *vs.* the commercially available **23**). This trend is also consistent with the results of the initial screening of the 35 fenarimol analogues, summarised in

Chapter 1.7.1, Figure 6. It must be noted that in most of these instances, compounds that lack the fluoro- group also have variations in other moieties that prevents a definitive conclusion. This observation merits further investigation in future work but such *in vitro* potency could arise from some metabolic stability that is conveyed to the compounds containing the fluorine atoms in specific positions.

The remaining compounds synthesised in the present project are being tested for *in vitro* efficacy at the time of writing and would address more questions regarding the correlation between chemical structures and potency (**Figure 11**, compounds "*currently being tested*"). Does the size of the carbamate substituent really have little effect on a compound's potency against *M. mycetomatis* (**Figure 11**, **15** and **16** *vs.* **17** and **18**)? Do substituents on the piperazine ring determine potency (**Figure 11**, **16** *vs.* **21** and **22**)? What will be the influence of the central alcohol on both potency and compound solubility when the hydroxyl is modified to another group (**Figure 11**, **10** *vs.* **11**, **12** and **13**)? Resolutions to these unanswered questions would pave a clear path for future synthesis in this project in the near term.

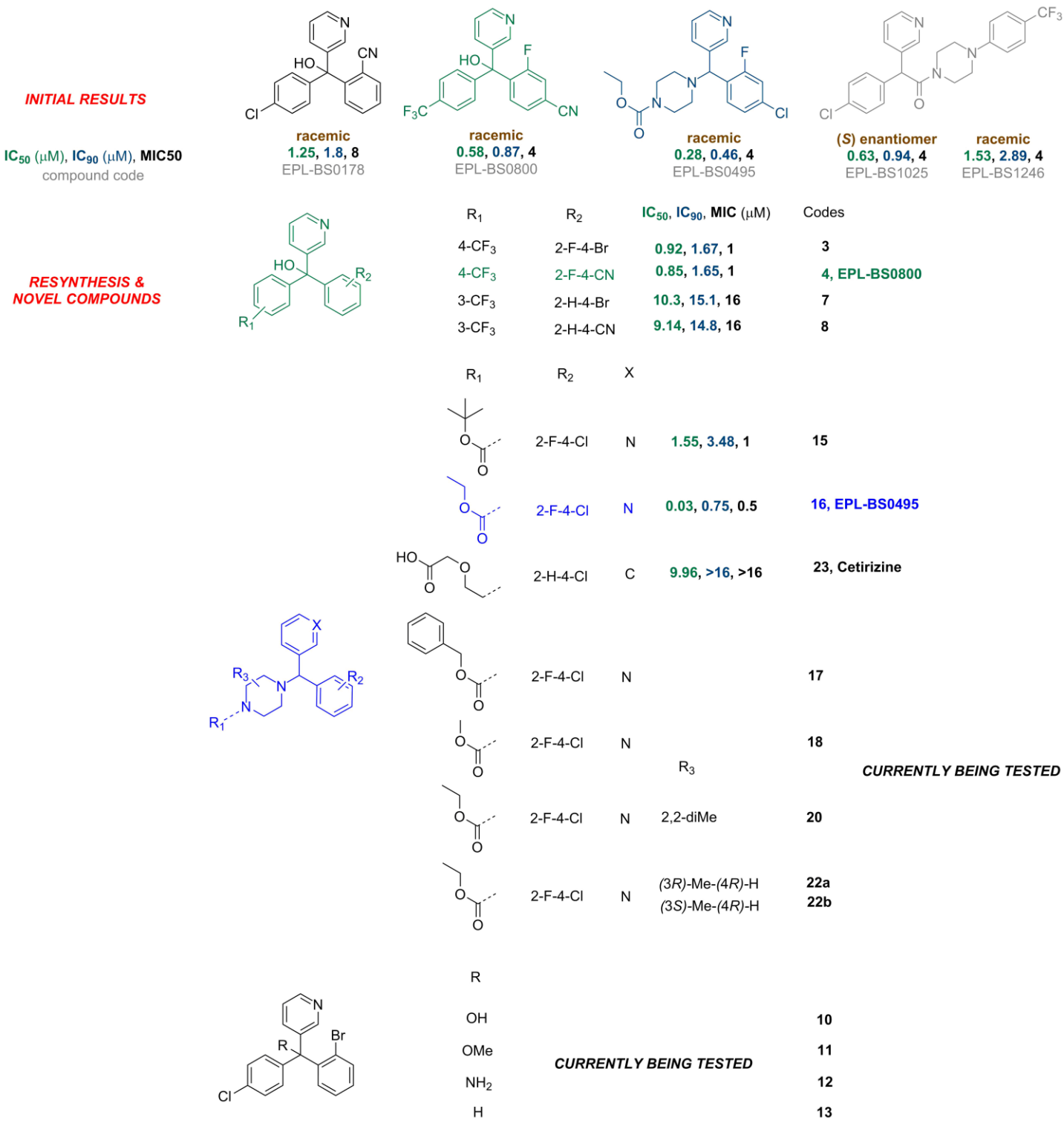

Figure 11: *In vitro* potency of fenarimol analogues against *M. mycetomatis*.

2.4.2. Larval Survival Results

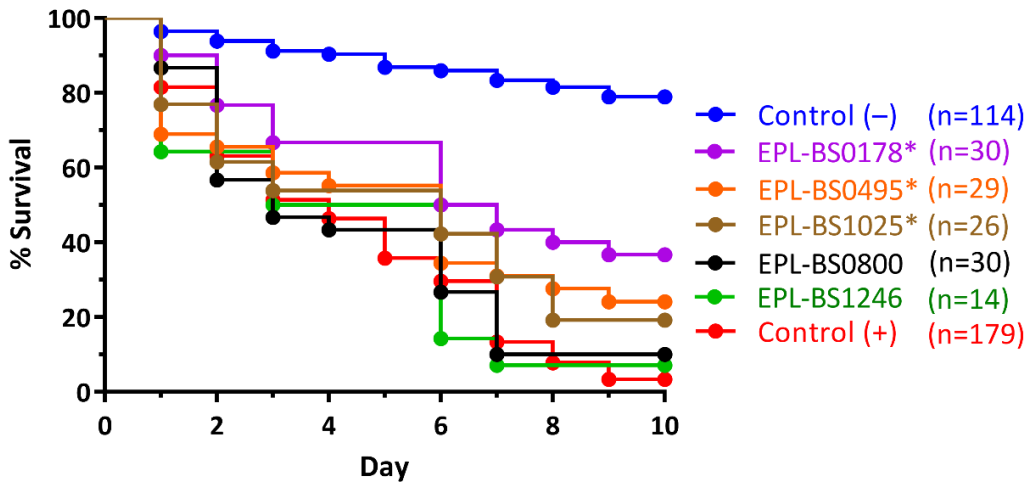

Figure 12: Survival of infected *G. mellonella larvae* when fenarimol analogues were administered (20 µM). Asterisks (*) denote a statistically significant survival rate compared to controls. Buffer PBS were injected to larvae that were uninfected (Control (–)) or infected with *M. mycetomatis* (Control (+)).

In the *in vivo* model of eumycetoma, larvae of the wax moth *Galleria mellonella* infected with *M. mycetomatis* were administered doses of each drug candidate and monitored over 10 days for survival. The pupation or death from injuries of some larvae were small limitations that were easily offset by statistically comparing results with negative controls (where uninfected larvae were administered a placebo buffer) and positive controls (where infected larvae were administered a placebo buffer). The compounds used in this *in vivo* assay were those used in the original screening of 35 fenarimol analogues; compounds synthesised in the present project have been submitted for, but not yet been evaluated with, the *in vivo* model. The raw *in vivo* data were obtained by Dr. Wendy van de Sande and has been used with permission.

Over 10 days, significant survival rates were observed for the treatment with EPL-BS0178 (37%), EPL-BS0495 (24%) and EPL-BS0800 (19%) (**Figure 12**). Despite having the most promising *in vitro* activity, EPL-BS0800 treatment resulted in a poor survival rate (10%) which could be explained by the fact that this compound is effective against the pathogen but cannot penetrate the grain layer *in vivo*.

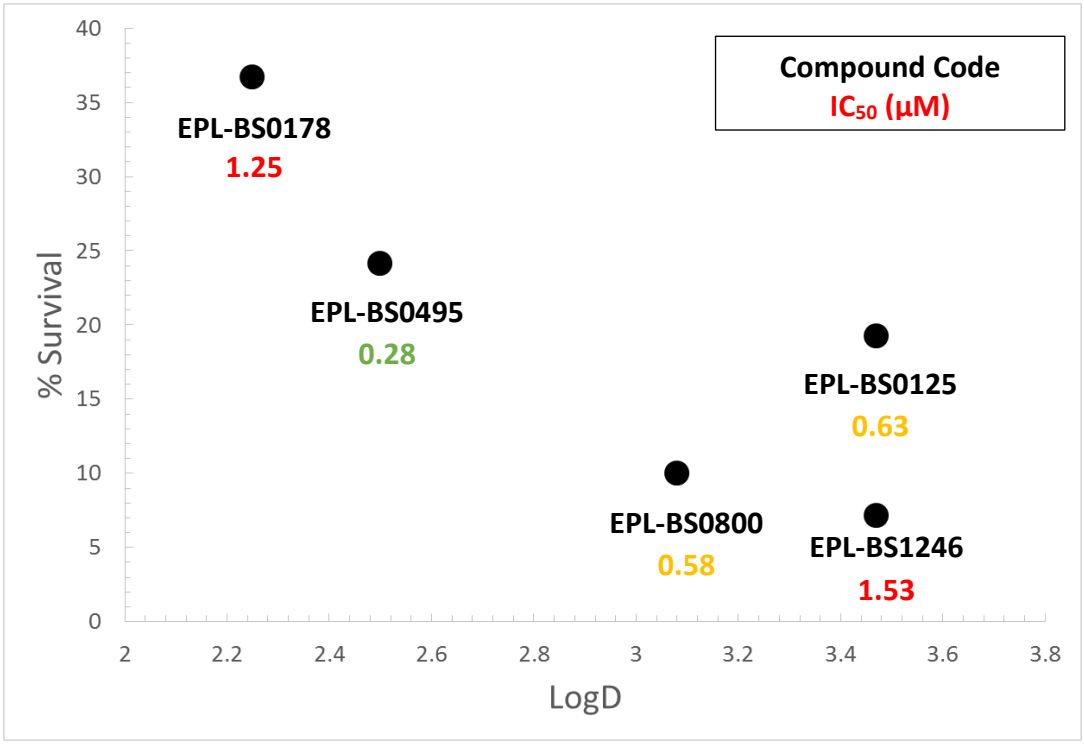

Figure 13: Comparison of larval survival with LogD of fenarimol analogues at physiological pH.

Interestingly, the LogD analysis of fenarimol analogues revealed that, in general, compounds with poor *in vivo* activity are more lipophilic (EPL-BS0800 and EPL-BS1246) while those with good *in vivo* potency are less lipophilic (EPL-BS0178 and EPL-BS0495) (**Figure 13**). This trend is independent of the *in vitro* results, which implies lipophilicity-correlated potency pertains to the *in vivo* model and possibly to the grain formation, though research in the identification of the grain compositions are needed for confirmation.

Chapter 3: Conclusion and Future Work

The successful resynthesis of EPL-BS0800 and EPL-BS0495 demonstrated the robustness of the reaction pathway to produce fenarimol analogues. Although EPL-BS0178 could not be synthesised, its precursor still exhibited comparable *in vitro* activity against eumycetoma.

With guidance from biological evaluation results, novel compounds were synthesised which showed a preliminary trend of chemical moieties with good and poor activity. More patterns will emerge once all of the biological results for the novel compounds are obtained.

The correlation between the *in vivo* activity and compound lipophilicity is particularly valuable because this result guides further target synthesis. Further information on the mycetoma grain composition will be crucial, in particular to guide the development of an *in vitro* grain assay that allows a determination of how well small molecules penetrate the grain structure.

While this present project was built on the concept of phenotypic drug discovery where the fast discovery of candidates against a target pathogen is favoured over the elucidation of a mechanism of action,[53] it is realised that, once a set of initial targets are obtained, the understanding of such mechanism will be greatly beneficial to the progress of drug discovery.[54] The fenarimol analogues explored in the present project were first synthesised as drug candidates for *Trypanosoma cruzi*. Fenarimol analogues inhibit the CYP51 protein which is required the biosynthesis and metabolism of *T. cruzi*.[16] Much less is known about the biology of *M. mycetomatis* but it is possible that the fenarimol analogues also have similar modes of action with *M. mycetomatis*.

Any future work involving the elucidation of mechanism of action for *M. mycetomatis* will be a collaboration with Dr. Wendy van de Sande. A library of resistant mutants will be generated by culturing *M. mycetomatis* in sublethal

doses of bioactive compounds and sequencing the pathogen's genome to determine the changes that bring about such resistance.[55] This knowledge would help prioritise synthesis of molecules that would not only target various strains of *M. mycetomatis* but do so *via* many different pathways, thus creating a powerful group of drug candidates.

The present project successfully established the online and digital framework which includes the use of *LabArchives* to efficiently store and share data as well as a *Reddit* community to show the general public the progress of drug discovery and inspire contributions. Such an open framework will serve a concrete foundation upon which Open Source Mycetoma will be built and with which the community can now be involved in the next stages of the project.

With the official project launch soon approaching, public inputs will generate interesting targets for synthesis and biological testing. The ongoing acquisition of biological activity against eumycetoma for a diverse range of candidates would also result in brand new chemical spaces to explore and optimise. The broader research community will be asked for two immediate inputs: i) samples of molecules structurally related to those in the present project but which are unpublished and ii) which of the remaining compounds in the large Epichem library ought to be evaluated next. By posing specific questions of this type it is expected that this research project will start the building of a community dedicated to finding new lead candidates for the treatment of one of the most neglected of the neglected tropical diseases.

Chapter 1: Experimental

1.1. General Experimental Details

Reagents were purchased from Sigma-Aldrich, Merck, Alfa Aesar, Matrix Scientific, Acros or 1-Click Chemistry. Unless otherwise specified, all reagents were used as purchased. Anhydrous conditions means glassware was heated under vacuum for 10 min, cooled and purged with nitrogen gas. Anhydrous solvents were collected freshly from a PureSolv MD7 solvent purification system where the solvents had passed through an anhydrous alumina column. Reactions at elevated temperature were achieved with a silicone oil bath with a temperature probe in the bath. Reactions at cold temperature were achieved with an ice bath (0°C) or acetone/dry ice bath (–78°C). Reduced pressure means rotary evaporation at 40°C (900–50 mbar). Analytical thin layer chromatography (TLC) was performed on Merck silica gel 60 F254 pre-coated aluminium plates (0.2 mm) and visualized under UV light (254 nm). Flash column chromatography was carried out on a Biotage Isolera Dalton using Merck silica gel 60 (0.040–0.063 mm).

1.2. General Spectroscopic Analysis Details

^{1}H and ^{13}C NMR spectra were obtained on either Bruker Avance DPX200 (200 MHz and 50 MHz respectively), DPX300 (300 MHz and 75 MHz respectively), DPX400 (400 MHz and 100 MHz respectively), DPX500 (500 MHz and 125 MHz respectively) or DPX600 (600 MHz and 150 MHz respectively) instruments. Spectra were processed using Bruker Topspin or Mestrelab Research Mnova. Deuterated solvents ($CDCl_3$, $(CD_3)_2CO$, D_2O) were obtained from Cambridge Isotope Laboratories. ^{1}H and ^{13}C chemical shifts are reported in parts per million (ppm) with respect to TMS at 0.00 ppm. The chemical shifts of the spectra were calibrated to residual solvent peaks (^{1}H: $CHCl_3$ 7.26 ppm, $(CH_3)_2CO$ 2.05 ppm, H_2O 4.79 ppm, TMS 0.00 ppm; ^{13}C: $CHCl_3$ 77.16 ppm, CH_3OH 49.00 ppm,

$(CH_3)_2CO$ 29.84 and 206.26 ppm, TMS 0.00 ppm). ^1H signal multiplicity is reported as: s = singlet, d = doublet, t = triplet, q = quartet and m = multiplet.

Coupling constants (*J*) are reported in Hertz (Hz). Integrals are relative. Low resolution mass spectrometry (m/z) was carried out on a Bruker amaZon SL quadrupole ion trap mass spectrometer using electrospray ionisation (ESI) or atmospheric-pressure chemical ionisation (APCI). High resolution mass spectrometry (HRMS) was performed on a Bruker 7T FT-ICR using ESI. Infrared (IR) spectra were recorded on a Bruker Platinum Alpha-E FTIR spectrometer. Samples were analysed neat. IR spectra are reported with frequency of maximum absorbance ν_{max} (cm^{-1}). Elemental analyses were carried out by Dr Christopher McRae at the Chemical Analysis Facility, Macquarie University on a Carlo Erba EA 1108 Elemental Analyser. Melting points (m.p.) were recorded on a Stanford Research Systems OptiMelt at 2°C per min (capillaries ø = 1.5–1.6 mm, 90 mm).

1.3. General Methods for Biological Evaluation

1.3.1. *In Vitro* Assay

The method for the *in vitro* assay was developed and provided by Dr. Wendy van de Sande.

M. mycetomatis was cultured for 7 days at 37˚C in RPMI 1640 medium supplemented with 0.3 g/L *L*-glutamine and 20 mM morpholinepropanesulfonic acid (MOPS). The mycelia were harvested by a centrifugation and homogenized by sonication for 20 s at 28 µm (Soniprep, Beun de Ronde, the Netherlands). The fungal suspension was diluted in RPMI 1640 medium to obtain a transmission of 70% at 660 nm (Novaspec II, Pharmacia Biotech). In each well of a 96-well microplate, 100 µL of suspension was added. Per well 1 µL of compound was added to obtain a final concentration of 100 µM. The microplate was taped to prevent evaporation and incubated for 7 days at 37°C. To facilitate end-point reading 2,3-bis(2-methoxy-4-nitro-5- sulfophenyl)-5-[(phenylamino)carbonyl]-2H-tetrazolium hydroxide (XTT) to a final concentration of 25 µg/well was added and incubated for 2 h at 37˚C and another 3 h at rt. Plates were

centrifuged and the extinction of 100 µL of supernatant was measured spectrophotometrically at 450 nm. Complete growth reduction was defined as 80% or more reduction in viable fungal mass. Each compound was tested in triplicate. To establish which compounds were most potent in inhibiting *M. mycetomatis* growth, the concentration at which growth reduction of 50% was obtained (IC_{50}) was determined. For this, all positive compounds were tested at concentrations of 0.098 µM, 0.39 µM, 1.56 µM, 6.25 µM and 25 µM. Growth was plotted against the concentration and the IC_{50} was determined from the resulting graphs.

To determine if the most potent compounds identified above were also active against *M. mycetomatis* isolates with a different genetic background, seven *M. mycetomatis* isolates with different AFLP types were selected. Minimal inhibitory concentrations (MIC) were determined using the same protocol as described above. Concentrations ranged from 0.007 µM to 32 µM.

1.3.2. *In Vivo* Assay

The method for the *in vivo* assay was developed and provided by Dr. Wendy van de Sande.

M. mycetomatis mycelia were cultured in colorless RPMI 1640 medium supplemented with L-glutamine (0.3 g/L), 20 mM morpholinepropanesulfonic acid (MOPS) and chloramphenicol (100 mg/L; Oxoid, Basingstroke, United Kingdom) for 2 weeks at 37°C and sonicated for 2 min at 28 micron. The resulting homogenous suspension was washed once in PBS and further diluted to an inoculum size of 4 mg wet weight per larvae. Inoculation was performed by injecting 40 µL of the fungal suspension in the last left pro-leg with an insulin 29G U-100 needle (BD diagnostics, Sparsk, USA). As controls larvae injected with PBS were included. Larvae were treated with 20 µM of compound per larvae. Compounds were administered 4 h, 28 h and 52 h after infection. Treatment was started at 4 h since at that time point grains were already visible. To monitor the course of infection, larvae were checked daily for survival for 10 days. If during these 10 days larvae formed pupa, these individuals were left out of the

equation, since we could not ascertain that these individual larvae would have survived or died during the infection.

1.4. General Methods for Chemical Synthesis

1.4.1. Method A, Lithiation

n-Butyllithium (1.5 equiv, 1.6 M solution in hexanes) was added dropwise to a solution of 3-bromopyridine (1.5 equiv) in dried diethyl ether at –78°C. After stirring for 30 min at –78°C, a solution of the 4-bromobenzaldehyde (1 equiv) in dried tetrahydrofuran was added. After stirring for 1 h at –78°C, the reaction was allowed to warm to –40°C, was quenched with a saturated solution of ammonium chloride and extracted with ethyl acetate. The organic phases were combined, dried ($MgSO_4$) and concentrated under reduced pressure.

1.4.2. Method B, Lithiation

n-Butyllithium (2 equiv, 1.6 M solution in hexanes) was added dropwise to a solution of 4-bromobenzotrifluoride (2 equiv) in dried diethyl ether at –78°C. The reaction mixture was stirred for 2 h. A solution of diarylmethanone (1 equiv) in dried tetrahydrofuran was added dropwise at –78°C. The reaction was allowed to warm to rt overnight, was quenched with water and extracted with ethyl acetate. The organic phases were combined, dried ($MgSO_4$) and concentrated under reduced pressure.

1.4.3. Method C, Diarylalcohol Oxidation

Activated manganese dioxide (3–7 equiv) was added to a solution of diarylalcohol (1 equiv) in DCM. After being heated at reflux for 4 h, the reaction mixture was cooled and filtered through celite. The filter cake was washed with DCM. The filtrate was concentrated under reduced pressure.

1.4.4. Method D, Cyanation

A mixture of bromo-substituted fenarimol (1 equiv), potassium hexacyanoferrate(II) trihydrate (2 equiv), palladium(II) acetate (0.2 equiv), anhydrous sodium carbonate (2 equiv) and anhydrous *N*,*N*-dimethylacetamide was heated under nitrogen at 130°C overnight. After cooling, the reaction mixture was quenched with water. The aqueous layer was extracted with ethyl acetate. The combined organic layers were washed with water, followed by brine, dried ($MgSO_4$) and concentrated under reduced pressure.

1.4.5. Method E, Nucleophilic Substitution

Thionyl chloride (2 equiv) was added to a solution of diarylalcohol (1 equiv) in DCM at 0°C. The reaction was allowed to warm to rt over 2 h, quenched with a saturated solution of sodium carbonate and extracted with DCM. The organic phases were combined, washed with brine, dried ($MgSO_4$) and concentrated under reduced pressure to give the aryl chloride intermediate, used without further purification. Anhydrous triethylamine (1.5 equiv) and dried potassium iodide (1 small spatula tip) were added to a solution of the aryl chloride intermediate and *tert*-butyl piperazine-1-carboxylate (1 equiv) in anhydrous acetonitrile. After being heated at 80°C for 48 h, the reaction was cooled and concentrated under reduced pressure. The concentrated residue was partitioned between DCM and a saturated solution of sodium carbonate. The aqueous layer was extracted with DCM. The organic layers were combined, dried ($MgSO_4$) and concentrated under reduced pressure to give a crude orange oil.

1.4.6. Method F, Acylation

TFA (10 equiv) was added to a solution of the Boc-piperazine compound (1 equiv) in DCM at 0°C. The reaction mixture was allowed to warm to rt overnight, concentrated under reduced pressure to give the crude TFA salt intermediate, used without further purification. Anhydrous triethylamine (25 equiv) and ethyl chloroformate (0.9 – 1 equiv) were added to a solution of the TFA salt

intermediate in DCM at 0°C. The reaction mixture was allowed to warm to rt overnight, quenched with a saturated solution of ammonium chloride and extracted with DCM. The organic layers were combined, dried ($MgSO_4$) and concentrated under reduced pressure.

1.5. Synthetic Procedure

1.5.1. (4-Bromo-2-fluorophenyl)(pyridin-3-yl)methanol, 1

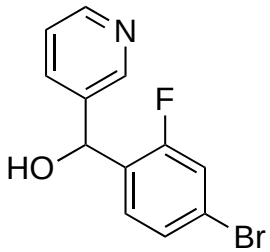

Prepared according to Method A, using 4-bromo-2-fluorobenzaldehyde (5.6 g, 0.027 mol) in tetrahydrofuran (20 mL) to give *the title compound* as a reddish brown waxy solid (7.3 g, 96%), used without further purification. **^{1}H NMR** (500 MHz, Acetone-d_6) δ 8.62 (d, *J* = 2.4 Hz, 1H), 8.46 (dd, *J* = 4.8, 1.7 Hz, 1H), 7.74 (dt, *J* = 7.9, 2.5, 1.3 Hz, 1H), 7.70 – 7.59 (m, 1H), 7.44 (dd, *J* = 8.4, 1.9 Hz, 1H), 7.37 – 7.24 (m, 2H), 6.13 (s, 1H). **^{19}F NMR** (471 MHz, Acetone-d_6) δ –116.62. **LRMS** *m/z* (ESI) 340 (87%), 338 (100%), 284 ([M+H]$^+$, 20%), 282 ([M+H]$^+$, 18%). **HRMS** (ESI) calcd. for $C_{12}H_{10}{}^{81}BrFNO^+$ 283.99093 and $C_{12}H_{10}{}^{79}BrFNO^+$ 281.99298 ([M+H]$^+$), found 283.99035, 281.99242. **IR** (film): ν_{max} 3123 (br), 2923, 2853, 1603, 1574, 1479, 1425, 1398 cm^{-1}. Spectroscopic data matched those in the literature.[16] However, literature characterisation was incomplete.

1.5.2. (4-Bromo-2-fluorophenyl)(pyridin-3-yl)methanone, 2

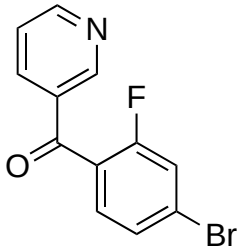

Prepared according to Method C, using activated manganese dioxide (5.8 g, 0.025 mol) and a solution of **1** (6.7 g, 0.076 mol) in DCM (55 mL). The crude mixture was purified by column chromatography to give *the title compound* as a cream solid (0.83 g, 12%) and recovered **1** as a reddish brown waxy solid (3.4 g, 50%). **^{1}H NMR** (500 MHz, Acetone-d_6) δ 8.98 – 8.93 (m, 1H), 8.84 (dd, *J* = 4.8, 1.7 Hz, 1H), 8.19 (dt, *J* = 8.0, 2.7, 1.4 Hz, 1H), 7.74 – 7.45 (m, 4H). **^{13}C NMR** (126 MHz, Acetone-d_6) δ 190.6, 160.0 (d, *J* = 255.7 Hz), 153.8, 150.4 (d, *J* = 1.7 Hz), 136.5, 132.8, 132.3 (d, *J* = 3.3 Hz), 128.3 (d, *J* = 3.7 Hz), 126.4

(d, *J* = 9.6 Hz), 125.3 (d, *J* = 14.5 Hz), 123.7, 120.0 (d, *J* = 25.2 Hz). **^{19}F NMR** (471 MHz, Acetone-d_6) δ –109.99. **LRMS** *m/z* (ESI) 340 (87%), 338 (100%), 304 ([M+Na]$^+$, 27%), 302 ([M+Na]$^+$, 21%), 282 ([M+H]$^+$, 27%), 280 ([M+H]$^+$, 23%). **HRMS** (ESI) calcd. for $C_{12}H_8{}^{81}BrFNO^+$ 281.97528 ([M+H]$^+$) and $C_{12}H_8{}^{79}BrFNO^+$ 279.97733, found 281.97476, 279.97677. **IR** (film): ν_{max} 3007, 1654 (s), 1584, 1417, 1395 cm^{-1}. **Anal.** cald. for $C_{12}H_7BrFNO$: C 51.46 H 2.52, N 5.00, found 51.35, 2.11, 4.89. Spectroscopic data matched those in the literature.[16] However, literature characterisation was incomplete.

1.5.3. (4-Bromo-2-fluorophenyl)(pyridin-3-yl)(4-(trifluoromethyl)phenyl)methanol, 3

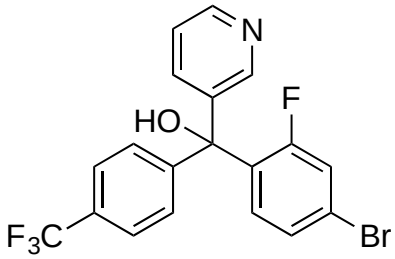

Prepared according to Method B, using 4-bromobenzotrifluoride (0.9 mL, 0.0054 mol) in diethyl ether (45 mL), *n*-butyllithium (3.8 mL, 1.6 M solution in hexanes, 0.0053 mol) and a solution of **2** (0.74 g, 0.0027 mol) in tetrahydrofuran (30 mL). The crude mixture was purified by column chromatography (ethyl acetate/hexane) to give *the title compound* as an orange solid (0.40 g, 35%). **m.p.** 167.1–169.0°C. **^{1}H NMR** (500 MHz, Acetone-d_6) δ 8.55 (s, 1H), 8.50 (d, *J* = 4.8, 1.6 Hz, 1H), 7.73 (d, *J* = 8.0 Hz, 3H), 7.62 (d, *J* = 8.2 Hz, 2H), 7.46 (d, *J* = 4.5 Hz, 1H), 7.41 – 7.29 (m, 2H), 6.09 (s, 1H). **^{13}C NMR** (126 MHz, Acetone-d_6) δ 160.6 (d, *J* = 252.7 Hz), 150.3, 149.7 (d, *J* = 2.2 Hz), 149.5, 141.4, 135.7 (d, *J* = 1.9 Hz), 133.6 (d, *J* = 11.4 Hz), 131.5 (d, *J* = 3.8 Hz), 130.0 (q, *J* = 32.1 Hz), 129.0 (d, *J* = 1.9 Hz), 128.4 (d, *J* = 3.3 Hz), 125.9 (q, *J* = 3.8 Hz), 125.3 (q, *J* = 271.3 Hz), 123.8, 123.0 (d, *J* = 9.5 Hz), 120.6 (d, *J* = 26.2 Hz), 78.7. **LRMS** *m/z* (ESI) 428 ([M+H]$^+$, 91%), 426 ([M+H]$^+$, 100%), 348 (22%), 340 (27%), 338 (32%), 333 (17%), 332 (24%). **HRMS** (ESI) calcd. for $C_{19}H_{13}{}^{81}BrF_4NO^+$ 428.00962 and $C_{19}H_{13}{}^{79}BrF_4NO^+$ 426.01166 ([M+H]$^+$), found 428.00934, 426.01138. **IR** (film): ν_{max} 3096 (br), 1601, 1567, 1477, 1419, 1324 cm^{-1}. Spectroscopic data matched those in the literature.[16] However, literature characterisation was incomplete. Due to limited amounts of material available, elemental analysis of this sample was performed once, rather than in duplicate. **Anal.** Results for carbon level in sample are above

tolerance values but the elemental analysis will be repeated on a freshly synthesized sample; cald.: C 53.54, H 2.84, N 3.29, found C 55.27, H 2.70, N 3.05.

1.5.4. 3-Fluoro-4-(hydroxy(pyridin-3-yl)(4-(trifluoromethyl)phenyl)methyl)benzonitrile, 4, EPL-BS0800

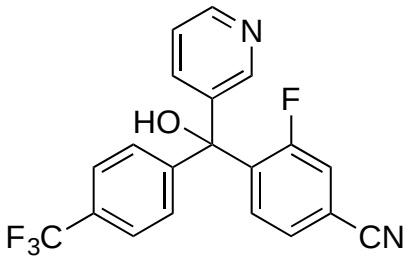

Prepared according to Method D, using **3** (0.20 g, 0.45 mmol), potassium hexacyanoferrate(II) trihydrate (0.42 g, 0.95 mmol), palladium acetate (0.031 g, 0.062 mmol), anhydrous sodium carbonate (0.057 g, 0.93 mmol) and anhydrous *N*,*N*-dimethylacetamide (2.3 mL). The crude product was purified with column chromatography (hexane/ethyl acetate) to obtain *the title compound* as a pale straw-coloured fine solid (55 mg, 32%). **m.p.** 129.5–132.1°C. **^{1}H NMR** (500 MHz, Acetone-d_6) δ 8.57 (d, *J* = 2.5 Hz, 1H), 8.53 (dd, *J* = 4.8, 1.6 Hz, 1H), 7.82 (t, *J* = 8.0 Hz, 1H), 7.77 – 7.69 (m, 4H), 7.66 – 7.58 (m, 3H), 7.38 (ddd, *J* = 8.1, 4.7, 0.8 Hz, 1H), 6.22 (s, 1H). **^{13}C NMR** (126 MHz, Acetone-d_6) δ 160.2 (d, *J* = 251.0 Hz), 149.8, 149.7 (d, *J* = 2.3 Hz), 140.8, 139.5 (d, *J* = 11.4 Hz), 135.7 (d, *J* = 2.1 Hz), 131.1 (d, *J* = 3.8 Hz), 130.4 (q, *J* = 32.2 Hz), 129.5 (d, *J* = 3.7 Hz), 129.0 (d, *J* = 1.9 Hz), 126.0 (q, *J* = 3.8 Hz), 125.2 (q, *J* = 271.2 Hz), 123.9, 121.0 (d, *J* = 26.8 Hz), 117.9 (d, *J* = 2.7 Hz), 114.6 (d, *J* = 10.0 Hz), 78.9 (1 obscured signal). **^{19}F NMR** (471 MHz, Acetone-d_6) δ –63.07, –104.20. **HRMS** (ESI) calcd. for $C_{20}H_{13}F_4N_2O^+$ 373.09640 ($[M+H]^+$), found 373.09610. **IR** (film): ν_{max} 3077 (br), 2241, 1617, 1562, 1490, 1411, 1325 cm^{-1}. Spectroscopic data matched those in the literature.[16] However, literature characterisation was incomplete. **Anal.** Results for carbon level in sample are above tolerance values but the elemental analysis will be repeated on a freshly synthesized sample; cald.: C 64.52, H 3.25, N 7.52 found C 49.49, H 0.86, N 5.30.

1.5.5. (4-Bromophenyl)(pyridin-3-yl)methanol, 5

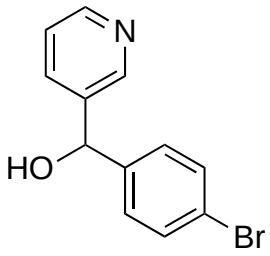

Prepared according to Method A, using 4-bromobenzaldehyde (10 g, 0.054 mol) to give *the title compound* as an orange solid (13 g, 95%), used without further purification. **^{1}H NMR** (500 MHz, Acetone-d_6) δ 8.63 (d, *J* = 2.3 Hz, 1H), 8.44 (dd, *J* = 4.7, 1.7 Hz, 1H), 7.77 – 7.69 (m, 1H), 7.55 – 7.47 (m, 2H), 7.44 – 7.36 (m, 2H), 7.30 (ddd, *J* = 7.8, 4.8, 0.9 Hz, 1H), 5.92 (s, 1H). **^{13}C NMR** (126 MHz, Acetone-d_6) δ 148.5, 148.3, 144.2, 140.2, 133.7, 131.3, 128.4, 123.2, 120.5, 72.5. **LRMS** *m/z* (ESI) 322 (100%), 320 (95%), 266 ([M+H]$^+$, 28%), 264 ([M+H]$^+$, 27%). **HRMS** (ESI) calcd. for $C_{12}H_{10}{}^{81}BrNONa^+$ 287.98230, $C_{12}H_{10}{}^{79}BrNONa^+$ 285.98435 ([M+Na]$^+$), found 287.98208, 285.98414. **IR** (film): ν_{max} 3149 (br), 2856, 1588, 1578, 1486, 1474, 1424, 1396 cm^{-1}. No spectroscopic data available for comparison.

1.5.6. (4-Bromophenyl)(pyridin-3-yl)methanone, 6

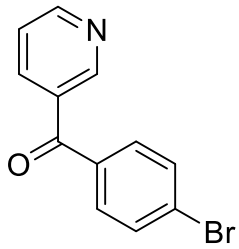

Prepared according to Method C, using activated manganese dioxide (21 g, 0.24 mol) and a solution of **5** (12 g, 0.045 mol) in DCM (75 mL). The crude mixture was purified by column chromatography to give *the title compound* as a cream solid (7.8 g, 69 %) and recovered **5** as an orange solid (1.4 g, 12%). **m.p.** 123.3–125.3°C. **^{1}H NMR** (500 MHz, Acetone-d_6) δ 8.94 (dd, *J* = 2.3, 0.9 Hz, 1H), 8.83 (dd, *J* = 4.9, 1.7 Hz, 1H), 8.15 (dt, *J* = 7.9, 2.0 Hz, 1H), 7.86 – 7.69 (m, 4H), 7.58 (ddd, *J* = 7.9, 4.8, 0.9 Hz, 1H). **^{13}C NMR** (126 MHz, Acetone-d_6) δ 193.5, 153.0, 150.4, 136.8, 136.0, 132.8, 131.9, 131.6, 127.4, 123.4. **LRMS** *m/z* (ESI) 286 ([M+Na]$^+$, 100%), 284 ([M+Na]$^+$, 79%), 264 ([M+H]$^+$, 45%), 262 ([M+H]$^+$, 44%). **HRMS** (ESI) calcd. for $C_{12}H_8{}^{81}BrNONa^+$ 285.96665 and $C_{12}H_8{}^{79}BrNONa^+$ 283.96870 ([M+Na]$^+$), found 285.96649, 283.96851. **IR** (film): ν_{max} 1650 (s), 1581, 1479, 1414, 1393, 1337 cm^{-1}. **Anal.** cald. for $C_{12}H_8BrNO$: C 54.99, H 3.08, N

5.34, found C 54.98, H 2.84, N 5.26. No spectroscopic data available for comparison.

1.5.7. (4-Bromophenyl)(pyridin-3-yl)(4-(trifluoromethyl)phenyl)methanol, 7

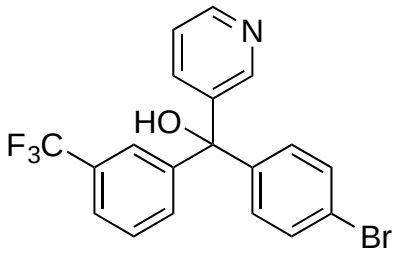

Prepared according to Method B, using 4-bromobenzotrifluoride (1.5 mL, 0.011 mol) in diethyl ether (145 mL), *N*-butyllithium (6.6 mL, 1.6 M solution in hexanes, 0.011 mol) and a solution of **6** (1.51 g, 0.0053 mol) in tetrahydrofuran (90 mL). The crude mix was purified by column chromatography (ethyl acetate/hexane) to give *the title compound* as a straw coloured solid (0.14 g, 5.8%) and recovered **6** as a cream solid (0.18g, 12.2%). **^{1}H NMR** (500 MHz, Acetone-d_6) δ 8.52 (dd, *J* = 2.5, 0.8 Hz, 1H), 8.50 (dd, *J* = 4.7, 1.6 Hz, 1H), 7.81 – 7.75 (m, 1H), 7.69 (tdd, *J* = 8.7, 2.6, 1.6 Hz, 2H), 7.63 – 7.48 (m, 4H), 7.36 (ddd, *J* = 8.0, 4.8, 0.9 Hz, 1H), 7.32 – 7.19 (m, 2H). **^{13}C NMR** (126 MHz, Acetone-d_6) δ 150.1, 149.5, 148.7 (d, *J* = 3.5 Hz), 146.5 (d, *J* = 3.9 Hz), 142.7 (d, *J* = 3.6 Hz), 136.0, 132.7, 132.0, 130.8, 130.7 (q, *J* = 31.9 Hz), 129.9, 125.3 (q, *J* = 271.6 Hz), 125.1 (q, *J* = 3.9 Hz), 124.9 (q, *J* = 4.0 Hz), 123.8, 122.1, 80.4 (d, *J* = 10.3 Hz). **^{19}F NMR** (471 MHz, Acetone-d_6) δ -63.04. **LRMS** *m/z* (ESI) 410 ([M+H]$^+$, 94%), 408 ([M+H]$^+$, 100%). **HRMS** (ESI) calcd. for $C_{19}H_{14}{}^{81}BrF_3NO^+$ 410.01904 and $C_{19}H_{14}{}^{79}BrF_3NO^+$ 408.02109 ([M+H]$^+$), found 410.01868, 408.02072. **IR** (film): ν_{max} 3066 (br), 2782, 1589, 1486, 1420, 1394, 1326 cm^{-1}. **Anal.** cald. C 67.8, H 3.70, N 7.84, found C 67.5, H 3.03, N 7.82. All data support isolation of a pure product, but the %H value is slightly outside tolerance limits that is not easily accounted for by typical solvent or water inclusion. This requires future investigation.

1.5.8. 4-(Hydroxy(pyridin-3-yl)(4-(trifluoromethyl)phenyl)methyl)benzonitrile, 8

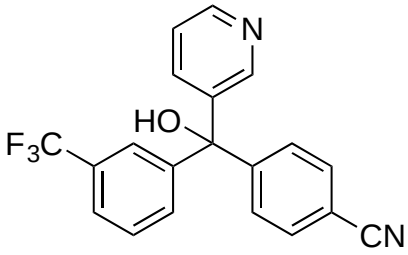

Prepared according to Method D, using **7** (150 mg, 0.42 mmol), potassium hexacyanoferrate(II) trihydrate (0.35 g, 0.79 mmol), palladium acetate (0.031 g, 0.062 mmol), anhydrous sodium carbonate (63 mg, 1.0 mmol) and anhydrous *N*,*N*-dimethylacetamide (1.8 mL). The crude product was purified with column chromatography (hexane/ethyl acetate) to obtain *the title compound* as a pale straw coloured fine solid (69 mg, 53%). **^{1}H NMR** (500 MHz, Acetone-d_6) δ 8.55 – 8.47 (m, 2H), 7.89 – 7.75 (m, 3H), 7.70 (ddd, *J* = 8.2, 4.2, 2.1 Hz, 2H), 7.66 – 7.47 (m, 4H), 7.37 (dd, *J* = 8.0, 4.8 Hz, 1H). **^{13}C NMR** (126 MHz, Acetone-d_6) δ 152.1 (d, *J* = 5.0 Hz), 150.1, 149.7, 148.1 (d, *J* = 5.1 Hz), 142.3 (d, *J* = 5.2 Hz), 136.1, 132.9, 132.7, 130.9 (q, *J* = 32.0 Hz), 130.0, 129.6, 125.3 (q, *J* = 3.8 Hz), 125.2 (q, *J* = 271.7 Hz), 124.9 (q, *J* = 3.9 Hz), 123.9, 119.1, 112.3, 80.5 (d, *J* = 10.8 Hz). **LRMS** *m/z* (ESI) 707 ($[2M–H]^-$, 88%), 353 ($[M–H]^-$, 100%). **HRMS** (ESI) calcd. for $C_{20}H_{14}F_3N_2O^+$ 355.10582, found 355.10543 ($[M+H]^+$). **IR** (film): ν_{max} 3055 (br), 2230 (w), 1606, 1592, 1578, 1501, 1476, 1420, 1327 cm^{-1}. No spectroscopic data available for comparison.

1.5.9. (2-Bromophenyl)(4-chlorophenyl)methanone, 9

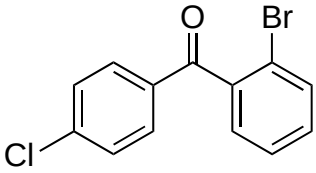

Aluminium chloride (19 g, 144 mmol, 1.5 equiv) was added portionwise to a mixture of 2-bromobenzoyl chloride (21 g, 96 mmol) and chlorobenzene (60 mL). The mixture was slowly warmed to 90°C and was heated at this temperature overnight. The mixture was allowed to cool to rt and was poured onto an excess of ice (600 mL) and aqueous hydrochloric acid (1 M, 450 mL). After 1 h, the resulting solution was extracted with DCM (2 × 600 mL), washed with aqueous hydrochloric acid (1 M, 2 × 450 mL), water (300 mL), aqueous sodium hydroxide (2 M, 2 × 450 mL) and water (300 mL), dried ($MgSO_4$) and concentrated under reduced pressure to give *the title compound* as a brown oil, used without further purification (28 g, 99%). **^{1}H NMR** (500 MHz,

Chloroform-*d*) δ δ 7.82 – 7.72 (m, 2H), 7.65 (d, *J* = 7.9, 1.1 Hz, 1H), 7.51 – 7.31 (m, 5H). **^{13}C NMR** (126 MHz, $CDCl_3$) δ 194.79, 140.46, 140.37, 134.67, 133.42, 131.66, 131.53, 129.18, 129.10, 127.49, 119.61, 77.16. **LRMS** *m/z* (ESI) 619 ([2M+Na]$^+$, 3%), 617 ([2M+Na]$^+$, 31%), 615 ([2M+Na]$^+$, 65%), 613 ([2M+Na]$^+$, 53%), 611 ([2M+Na]$^+$, 26%), 321 ([M+Na]$^+$, 22%), 319 ([M+Na]$^+$, 100%), 317 ([M+Na]$^+$, 81%). **IR** (film): ν_{max} 3086, 3053, 1662 (s), 1583, 1570, 1486, 1463 cm^{-1}. **HRMS** $C_{13}H_8{}^{81}Br^{37}ClONa$ 320.92948, $C_{13}H_8{}^{81}Br^{35}ClONa$ 318.93243, $C_{13}H_8{}^{79}Br^{37}ClONa$ 318.93152, $C_{13}H_8{}^{79}Br^{35}ClONa$ 316.93447 ([M+H]$^+$) found 320.92942, 318.93250, 316.93451. Spectroscopic data matched those in the literature.[34] However, literature characterisation was incomplete.

1.5.10. (2-Bromophenyl)(4-chlorophenyl)(pyridin-3-yl)methanol, 10

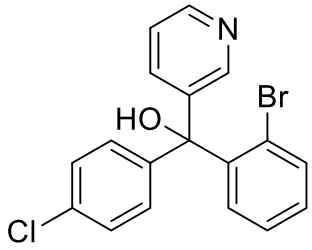

Prepared according to Method B, using bromopyridine (2.95 mL, 30 mmol), *n*-butyllithium (12.5 mL, 20 mmol) and **9** (3.0 g, 10 mmol). The reaction was allowed to proceed for 2 h at –78°C then quenched with water at –78°C. The crude product was purified by column chromatography (ethyl acetate/hexane) to give *the title compound* as a pale straw-coloured fine solid (2.3 g, 62%) and recovered **9** as a brown oil (0.34 g, 11%). **m.p.** 64.7–65.8°C. **^{1}H NMR** (500 MHz, Acetone-d_6) δ 8.86 – 8.19 (m, 2H), 7.83 – 7.55 (m, 2H), 7.48 – 7.24 (m, 7H), 7.12 (dd, *J* = 7.8, 1.9 Hz, 1H). **^{13}C NMR** (126 MHz, Acetone-d_6) δ 150.17, 149.07, 145.10, 145.00, 141.92, 136.29, 136.10, 133.62, 131.90, 130.67, 130.56, 128.85, 128.03, 124.00, 123.63, 81.57. **LRMS** *m/z* (ESI) 511 (29%), 509 (100%), 453 (24%), 451 (58%), 378 ([M+H]$^+$, 19%), 376 ([M+H]$^+$, 87%), 374 ([M+H]$^+$, 69%). **HRMS** (ESI) calcd. for $C_{18}H_{14}{}^{81}Br^{37}ClNO^+$ 377.98973, $C_{18}H_{14}{}^{81}Br^{35}ClNO^+$ 375.99268, $C_{18}H_{14}{}^{79}Br^{37}ClNO^+$ 375.99178 and $C_{18}H_{14}{}^{79}Br^{35}ClNO^+$ 373.99473 ([M+H]$^+$), found 377.98918, 375.99205, 373.99418. **IR** (film): ν_{max} 3057 (br), 2775, 1734, 1586, 1487, 1462, 1419, 1399 cm^{-1}. **Anal.** Sample has been sent at time of writing. Result pending. No spectroscopic data available for comparison.

1.5.11. 3-((2-Bromophenyl)(4-chlorophenyl)(methoxy)methyl)pyridine, 11

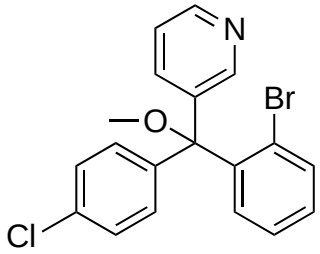

Compound **10** (100 mg, 0.31 mmol) in THF (2 mL) was slowly added to a suspension of sodium hydride (60% w/w in mineral oil, 23 mg, 0.935 mmol) in THF (5 mL) at 0°C. After 1 h at 0°C, iodomethane (0.03 mL, 0.47 mmol) was added and the mixture was allowed to warm to rt overnight. The mixture was quenched with water and extracted with diethyl ether. The organic layers were combined, dried ($MgSO_4$) and concentrated under reduced pressure. The crude product was purified with column chromatography (ethyl acetate/hexane) to give *the title compound* as a pale straw-coloured oil (34 mg, 33%). **^{1}H NMR** (500 MHz, Acetone-d_6) δ 8.76 – 8.57 (m, 1H), 8.46 (dd, *J* = 4.7, 1.5 Hz, 1H), 7.80 (m, 2H), 7.68 (dd, *J* = 7.9, 1.3 Hz, 1H), 7.57 – 7.09 (m, 7H), 3.11 (s, 3H). **^{13}C NMR** (126 MHz, Acetone-d_6) δ 150.4, 149.0, 141.9, 140.7, 139.1, 136.7, 136.2, 133.5, 132.7, 131.0, 130.8, 128.9, 128.3, 124.5, 123.6, 87.0, 53.0. **LRMS** *m/z* (ESI) 414 ([M+Na]$^+$, 6%), 412 ([M+Na]$^+$, 32%), 410 ([M+Na]$^+$, 29%), 392 ([M+H]$^+$, 29%), 390 ([M+H]$^+$, 100%), 388 ([M+H]$^+$, 70%). **HRMS** (ESI) calcd. for $C_{19}H_{15}{}^{81}Br^{37}ClNONa^+$ 413.98733, $C_{19}H_{15}{}^{81}Br^{35}ClNONa^+$ 411.98937, $C_{19}H_{15}{}^{79}Br^{37}ClNONa^+$ 411.99028 and $C_{19}H_{15}{}^{79}Br^{35}ClNONa^+$ 409.99232 ([M+Na]$^+$), found 413.98710, 411.99012, 409.99208. **IR** (film): ν_{max} 3057, 2937, 2827, 1702, 1488, 1417 cm^{-1}. No spectroscopic data available for comparison.

1.5.12. (2-Bromophenyl)(4-chlorophenyl)(pyridin-3-yl)methanamine, 12

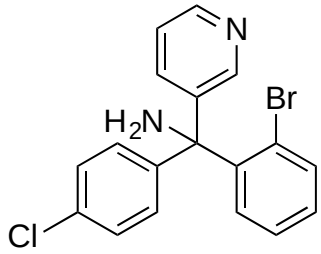

Thionyl chloride (0.15 ml, 1.5 mmol) was added to a solution of **10** (98 mg, 0.30 mmol) in dry DCM (10 ml) at 0°C. The mixture was allowed to warm to rt overnight then concentrated under reduced pressure.

Ammonia (7 N in MeOH) (0.35 mL, 2.3 mmol) was added to the residue in DCM (10 mL) at 0°C and the mixture was allowed to warm to rt for 48 h. The reaction was quenched with water and extracted with DCM. The organic layers were combined, dried ($MgSO_4$) and concentrated under reduced pressure. The crude product was purified with column chromatography (ethyl acetate/hexane) to give *the title compound* as a pale straw-coloured oil (33 mg, 34%). **^{1}H NMR** (500 MHz, Acetone-d_6) δ 8.67 – 8.38 (m, 2H), 7.89 – 7.60 (m, 2H), 7.43 – 7.13 (m, 7H), 7.04 – 6.63 (m, 1H), 3.19 (s, 2H). **^{13}C NMR** (126 MHz, Acetone-d_6) δ 150.5, 148.7, 147.1, 146.3, 136.5, 136.1, 133.2, 131.8, 130.7, 130.0, 128.9, 128.1, 123.9, 67.0 (2 obscured signals). **LRMS** *m/z* (ESI) 399 ([M+Na]$^+$, 12%), 397 ([M+Na]$^+$, 42%), 395 ([M+Na]$^+$, 33%), 377 ([M+H]$^+$, 27%), 375 ([M+H]$^+$, 100%), 373 ([M+H]$^+$, 77%). **HRMS** (ESI) calcd. for $C_{18}H_{15}{}^{81}Br^{37}ClN_2{}^+$ 377.00572, $C_{18}H_{15}{}^{81}Br^{35}ClN_2{}^+$ 375.00867, $C_{18}H_{15}{}^{79}Br^{37}ClN_2{}^+$ 375.00776, $C_{18}H_{15}{}^{79}Br^{35}ClN_2{}^+$ 373.01071 ([M+H]$^+$), found 377.00517, 375.00804, 373.01017. **IR** (film): ν_{max} 3058, 2937, 2828, 1701, 1584, 1572, 1487, 1416 cm^{-1}. No spectroscopic data available for comparison.

1.5.13. 3-((2-Bromophenyl)(4-chlorophenyl)methyl)pyridine, 13

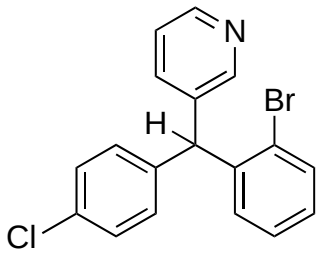

Sodium borohydride (0.53 g, 14 mmol) was cautiously added to TFA (10 mL) at 0°C. After 1.5 h at 0°C, a solution of **10** (81 mg, 0.25 mmol) in DCM (10 mL) was added portionwise. After 30 min at 0°C, the reaction was poured onto 25% aqueous sodium hydroxide/ice (35 mL) and extracted with diethyl ether (2 × 25 mL). The organic layers were combined, dried ($MgSO_4$) and concentrated under reduced pressure. The crude product was purified with column chromatography (ethyl acetate/hexane) to give *the title compound* as a pale straw-coloured oil (49 mg, 63%). **^{1}H NMR** (500 MHz, Acetone-d_6) δ 8.48 (dd, *J* = 4.7, 1.6 Hz, 1H), 8.39 (dt, *J* = 2.4, 0.8 Hz, 1H), 7.67 (dd, *J* = 8.0, 1.3 Hz, 1H), 7.48 – 7.42 (m, 1H), 7.41 – 7.30 (m, 4H), 7.27 – 7.21 (m, 1H), 7.18 – 7.09 (m, 2H), 7.05 – 6.53 (m, 1H), 6.02 (s, 1H). **^{13}C NMR** (126 MHz, Acetone-d_6) δ 151.7, 148.9, 142.7, 141.6, 138.5, 137.3, 134.2, 133.1, 132.0, 129.8, 129.5, 128.7, 125.7, 124.3, 53.8. **LRMS** *m/z* (ESI) 447 (25%), 446 (100%), 362

([M+H]$^+$, 6%), 360 ([M+H]$^+$, 27%), 358 ([M+H]$^+$, 21%). **HRMS** (ESI) calcd. for $C_{18}H_{13}{}^{81}Br^{37}ClNNa^+$ 383.97676, $C_{18}H_{13}{}^{81}Br^{35}ClNNa^+$ 381.97971, $C_{18}H_{13}{}^{79}Br^{37}ClNNa^+$ 381.97881, $C_{18}H_{13}{}^{79}Br^{35}ClNNa^+$ 379.98176, ([M+Na]$^+$), found 383.97684, 381.97973, 379.98176. **IR** (film): ν_{max} 3057, 3029, 2923, 2853, 1701, 1574, 1489, 1465, 1421 cm^{-1}. No spectroscopic data available for comparison.

1.5.14. (4-Chloro-2-fluorophenyl)(pyridin-3-yl)methanol, 14

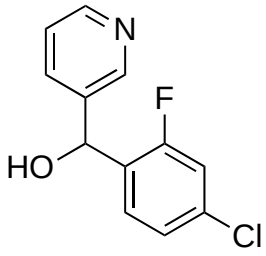

Prepared according to Method A, using 4-chloro-2-fluorobenzaldehyde (4.4 g, 0.027 mol) to give *the title compound* as a reddish orange waxy solid (5.6 g, 88%), used without further purification. **^{1}H NMR** (500 MHz, Acetone-d_6) δ 8.62 (d, *J* = 2.4 Hz, 1H), 8.46 (dd, *J* = 4.7, 1.7 Hz, 1H), 7.92 – 7.57 (m, 2H), 7.51 – 7.26 (m, 2H), 7.20 (m, 1H), 6.14 (s, 1H). **^{13}C NMR** (126 MHz, Acetone-d_6) δ 160.3 (d, *J* = 248.7 Hz), 149.6, 149.2 (d, *J* = 1.6 Hz), 139.9, 134.6, 134.3 (d, *J* = 10.5 Hz), 131.7 (d, *J* = 13.7 Hz), 129.9 (d, *J* = 5.2 Hz), 125.7 (d, *J* = 3.6 Hz), 124.2, 116.6 (d, *J* = 25.4 Hz), 67.6. **^{19}F NMR** (471 MHz, Acetone-d_6) δ –116.82. **LRMS** *m/z* (ESI) 296 (27%), 294 (100%), 240 ([M+H]$^+$, 2%), 238 ([M+H]$^+$, 8%). **HRMS** (ESI) calcd. for $C_{12}H_{10}{}^{37}ClFNO^+$ 240.04054 and $C_{12}H_{10}{}^{35}ClFNO^+$ 238.04350 ([M+H]$^+$), found 240.04000, 238.04295. **IR** (film): ν_{max} 3113 (br), 2929, 1609, 1578, 1482, 1426, 1402 cm^{-1}. No spectroscopic data available for comparison.

1.5.15. *tert*-Butyl 4-((4-chloro-2-fluorophenyl)(pyridin-3-yl)methyl)piperazine-1-carboxylate, 15

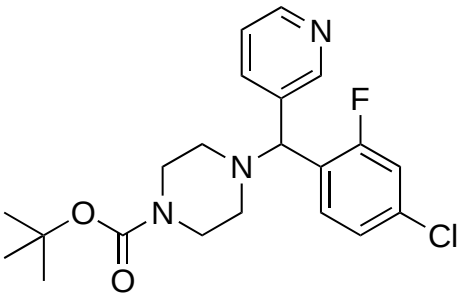

Prepared according to Method E, using thionyl chloride (3.6 mL, 0.047 mol) to give the aryl chloride intermediate **14a** as a crude brown oil (3.3 g, 66%), used without further purification. Continued according to Method E using anhydrous triethylamine (3.6 mL, 0.026 mol), dried potassium iodide (catalytic amount) and a solution of **14a** (3.0 g) and *tert*-butyl piperazine-1-carboxylate (3.6 g, 0.019 mol) in anhydrous acetonitrile (25 mL) to give a crude orange oil that was purified by column chromatography (ethyl acetate/hexane) to give *the title compound* as an amber resin (3.5 g, 75%). **^{1}H NMR** (200 MHz, Chloroform-*d*) δ 8.59 (d, *J* = 2.2 Hz, 1H), 8.41 (dd, *J* = 4.8, 1.6 Hz, 1H), 7.64 (dt, *J* = 7.9, 2.0 Hz, 1H), 7.46 (t, *J* = 8.0 Hz, 1H), 7.16 (ddd, *J* = 7.9, 4.8, 0.9 Hz, 1H), 7.12 – 6.99 (m, 1H), 6.96 (dd, *J* = 9.9, 2.1 Hz, 1H), 4.64 (s, 1H), 3.38 (t, *J* = 5.1 Hz, 4H), 2.69 – 2.18 (m, 4H), 1.38 (s, 9H). **^{13}C NMR** (75 MHz, Chloroform-*d*) δ 160.3 (d, *J* = 250.1 Hz), 154.6, 149.6, 148.9, 136.3, 135.4, 133.8 (d, *J* = 10.5 Hz), 129.5 (d, *J* = 4.7 Hz), 126.8 (d, *J* = 12.7 Hz), 125.1 (d, *J* = 3.4 Hz), 123.6, 116.5 (d, *J* = 26.1 Hz), 79.6, 64.3, 51.4, 28.4 (1 obscured signal). **LRMS** 430 ([M+Na]$^{+}$, 35%), 428 ([M+Na]$^{+}$, 100%), 408 ([M+H]$^{+}$, 7%), 406 ([M+H]$^{+}$, 19%). **HRMS** (ESI) calcd. for $C_{21}H_{25}{}^{37}ClFN_3O_2Na^{+}$ 430.14875 and $C_{21}H_{25}{}^{35}ClFN_3O_2Na^{+}$ 428.15170 ([M+Na]$^{+}$), found 430.14882, 428.15181. **IR** (film): ν_{max} 2974, 2814, 1688 (s), 1608, 1578, 1480, 1420, 1365 cm^{-1}. No spectroscopic data available for comparison.

1.5.16. Ethyl 4-((4-chloro-2-fluorophenyl)(pyridin-3-yl)methyl)piperazine-1-carboxylate, 16

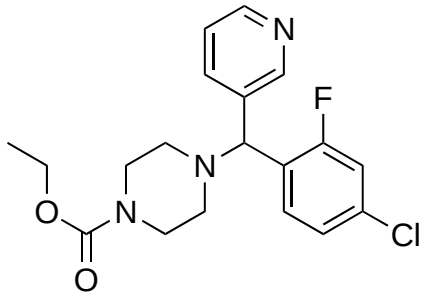

Prepared according to Method F, using TFA (6 mL, 0.080 mol) and **15** (3.2 g, 0.0078 mol) in DCM (35 mL) at 0°C to give the TFA salt intermediate **15a** (6.4 g) as a brown azeotrope with DCM, used without further purification. Continued according to Method F using anhydrous triethylamine (25 mL, 0.18 mol), ethyl chloroformate (0.75 mL 0.0075 mol) and a solution of **15a** (6.4 g) in DCM (50 mL). The crude product was purified with column chromatography (ethyl acetate/hexane) to give *the title compound* as an amber resin (2.0 g, 65%). **^{1}H NMR** (500 MHz, Chloroform-*d*) δ 8.63 (d, *J* = 2.2 Hz, 1H), 8.47 (dd, *J* = 4.8, 1.6 Hz, 1H), 7.68 (dt, *J* = 7.9, 2.0 Hz, 1H), 7.50 (t, *J* = 8.0 Hz, 1H), 7.22 (ddd, *J* = 7.9, 4.7, 0.8 Hz, 1H), 7.13 (dd, *J* = 8.4, 2.0 Hz, 1H), 7.03 (dd, *J* = 9.9, 2.1 Hz, 1H), 4.69 (s, 1H), 4.10 (q, *J* = 7.1 Hz, 2H), 3.47 (t, *J* = 5.1 Hz, 4H), 2.55 – 2.07 (m, 4H), 1.22 (t, *J* = 7.1 Hz, 3H). **^{13}C NMR** (126 MHz, Chloroform-*d*) δ 160.4 (d, *J* = 250.0 Hz), 155.5, 149.8, 149.1, 136.4, 135.5, 134.0 (d, *J* = 10.6 Hz), 129.6 (d, *J* = 4.7 Hz), 126.8 (d, *J* = 12.8 Hz), 125.2 (d, *J* = 3.5 Hz), 123.8, 116.7 (d, *J* = 26.0 Hz), 64.4 (d, *J* = 1.7 Hz), 61.5, 51.5, 43.8, 14.8. **LRMS** *m/z* (ESI) 402 ([M+Na]$^{+}$, 37%), 400 ([M+Na]$^{+}$, 100%). **HRMS** (ESI) calcd. for $C_{19}H_{21}{}^{37}ClFN_3O_2Na^{+}$ 402.11745 and $C_{19}H_{21}{}^{35}ClFN_3O_2Na^{+}$ 400.12040 ([M+Na]$^{+}$), found 402.11709 and 400.12007. **IR** (film): ν_{max} 2923, 2853, 1603, 1574, 1479, 1425, 1398 cm^{-1}. No spectroscopic data available for comparison.

1.5.17. Benzyl 4-((4-chloro-2-fluorophenyl)(pyridin-3-yl)methyl)piperazine-1-carboxylate, 17

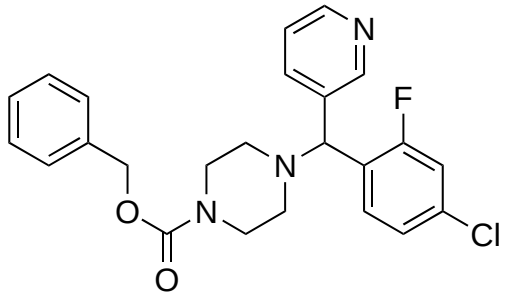

Prepared according to Method F, using TFA (0.9 mL, 12 mmol) and **15** (0.36 g, 0.9 mmol) in DCM (5 mL), anhydrous triethylamine (2.5 mL, 18 mmol), benzyl chloroformate (0.11 mL 0.78 mmol). The crude product was purified with column chromatography (ethyl acetate/hexane) to give *the title compound* as an amber resin (0.22 g, 63%). **^{1}H NMR** (600 MHz, Chloroform-*d*) δ 8.56 (s, 1H), 8.46 – 8.17 (m, 1H), 7.60 (d, *J* = 8.0 Hz, 1H), 7.41 (t, *J* = 8.0 Hz, 1H), 7.28 – 7.17 (m, 4H), 7.13 (dd, *J* = 7.9, 4.7 Hz, 1H), 7.04 (dd, *J* = 8.5, 2.0 Hz, 1H), 6.93 (dd, *J* = 9.9, 2.1 Hz, 1H), 5.03 (s, 2H), 4.61 (s, 1H), 3.73 – 3.01 (m, 4H), 2.67 – 1.93 (m, 4H). **^{13}C NMR** (151 MHz, Chloroform-*d*) δ 160.3 (d, *J* = 250.1 Hz), 155.1, 149.5, 148.9, 136.6, 136.3, 135.5, 133.9 (d, *J* = 10.5 Hz), 129.5 (d, *J* = 4.5 Hz), 128.5, 128.0, 127.8, 126.6 (d, *J* = 12.5 Hz), 125.1 (d, *J* = 3.5 Hz), 123.7, 116.6 (d, *J* = 26.0 Hz), 67.1, 64.3 (d, *J* = 1.6 Hz), 51.3, 43.8. **LRMS** *m/z* (ESI) 464 ([M+Na]$^+$, 39%), 462 ([M+Na]$^+$, 100%), 442 ([M+H]$^+$, 12%), 440 ([M+H]$^+$, 28%). **HRMS** (ESI) calcd. for $C_{24}H_{23}{}^{37}ClFN_3O_2Na^+$ 464.13310 and $C_{24}H_{23}{}^{35}ClFN_3O_2Na^+$ 462.13605 ([M+Na]$^+$), found 464.13334, 462.13624. **IR** (film): ν_{max} 2817, 1695 (s), 1607, 1577, 1481, 1426 cm^{-1}. No spectroscopic data available for comparison.

1.5.18. Methyl 4-((4-chloro-2-fluorophenyl)(pyridin-3-yl)methyl)piperazine-1-carboxylate, 18

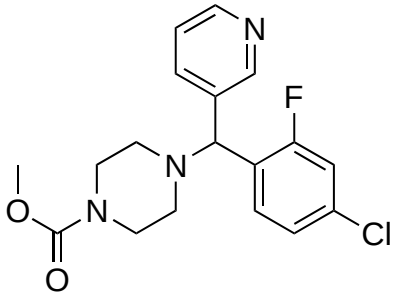

Prepared according to Method F, using TFA (0.9 mL, 12 mmol) and **15** (0.36 g, 0.9 mmol) in DCM (5 mL), anhydrous triethylamine (2.5 mL, 18 mmol), benzyl chloroformate (0.060 mL 0.77 mmol). The crude product was purified with column chromatography (ethyl acetate/hexane) to give *the title compound* as an amber resin (0.17 g, 61%). **^{1}H NMR** (600 MHz,

Chloroform-*d*) δ 8.62 (d, *J* = 2.1 Hz, 1H), 8.45 (dd, *J* = 5.0, 1.6 Hz, 1H), 7.67 (dd, *J* = 8.0, 2.0 Hz, 1H), 7.48 (t, *J* = 8.0 Hz, 1H), 7.21 (ddd, *J* = 7.9, 4.9, 0.8 Hz, 1H), 7.15 – 7.08 (m, 1H), 7.01 (dd, *J* = 9.9, 2.1 Hz, 1H), 4.68 (s, 1H), 3.65 (s, 3H), 3.46 (s, 4H), 2.69 – 2.05 (m, 4H). **^{13}C NMR** (151 MHz, Chloroform-*d*) δ 160.4 (d, *J* = 250.0 Hz), 155.8, 149.6, 148.9, 136.3, 135.6, 134.0 (d, *J* = 10.5 Hz), 129.5 (d, *J* = 4.8 Hz), 126.7 (d, *J* = 12.8 Hz), 125.2 (d, *J* = 3.6 Hz), 123.8, 116.7 (d, *J* = 26.0 Hz), 64.4, 52.7, 51.4, 43.8. **LRMS** *m/z* (ESI) 388 ([M+Na]$^+$, 36%), 386 ([M+Na]$^+$, 100%), 366 ([M+H]$^+$, 12%), 364 ([M+H]$^+$, 32%). **HRMS** (ESI) calcd. for $C_{18}H_{19}{}^{37}ClFN_3O_2Na^+$ 388.10180 and $C_{18}H_{19}{}^{35}ClFN_3O_2Na^+$ 386.10475 ([M+Na]$^+$), found 388.10185, 386.10483. **IR** (film): ν_{max} 2958, 2816, 1697 (s), 1607, 1578, 1472, 1444, 1408 cm^{-1}. No spectroscopic data available for comparison.

1.5.19. *tert*-Butyl 4-((4-chloro-2-fluorophenyl)(pyridin-3-yl)methyl)-2,2-dimethylpiperazine-1-carboxylate, 19

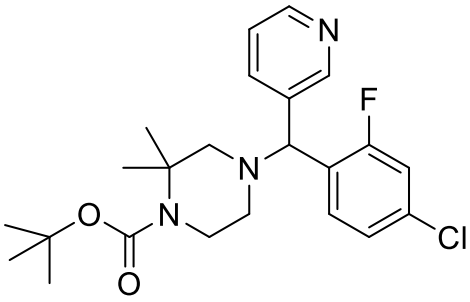

Prepared according to Method E, using **14** (2.8 g, 12 mmol) in DCM (55 mL) and thionyl chloride (1.7 mL, 23 mmol) to give the intermediate **14a** as a brown oil (2.4 g, 82%). Continued according to Method E using anhydrous triethylamine (0.7 mL, 5.1 mmol), dried potassium iodide (catalytic amount) and a solution of **14a** (0.66 g) and *tert*-butyl 2,2-dimethylpiperazine-1-carboxylate (3.6 g, 4.3 mmol) in anhydrous acetonitrile (4.5 mL) to give a crude orange oil that was purified with column chromatography (ethyl acetate/hexane) to give *the title compound* as an amber resin (0.70 g, 64%). **^{1}H NMR** (500 MHz, Chloroform-*d*) δ 8.64 (d, *J* = 2.2 Hz, 1H), 8.46 (dd, *J* = 4.8, 1.7 Hz, 1H), 7.70 (dt, *J* = 7.9, 2.0 Hz, 1H), 7.54 (t, *J* = 8.0 Hz, 1H), 7.22 (ddd, *J* = 7.9, 4.7, 0.8 Hz, 1H), 7.15 – 7.08 (m, 1H), 7.02 (dd, *J* = 9.9, 2.1 Hz, 1H), 4.58 (s, 1H), 3.64 – 3.15 (m, 2H), 2.55 – 2.35 (m, 2H), 2.24 – 2.08 (m, 2H), 1.43 (s, 9H), 1.37 (d, *J* = 1.8 Hz, 6H). **^{13}C NMR** (126 MHz, Chloroform-*d*) δ 160.4 (d, *J* = 249.9 Hz), 156.4, 149.7, 149.1, 136.6, 135.4, 133.9 (d, *J* = 10.5 Hz), 129.3 (d, *J* = 4.7 Hz), 127.3 (d, *J* = 12.7 Hz), 123.8, 116.7 (d, *J* = 25.9 Hz), 79.9, 65.0, 64.1 (d, *J* = 1.6 Hz), 54.9, 51.7, 43.0, 28.6, 25.3, 25.0. **LRMS** *m/z* (APCI) 436

([M+H]$^+$, 25%), 434 ([M+H]$^+$, 66%), 380 ([M–(C_4H_9)$^+$+2H$^+$]$^+$, 47%), 378 ([M–(C_4H_9)$^+$+2H$^+$]$^+$, 100%), 336 ([M–($C_5H_9O_2$)$^+$+2H$^+$]$^+$, 12%), 334 ([M–($C_5H_9O_2$)$^+$+2H$^+$]$^+$, 38%), 222 ([M–($C_{11}H_{21}N_2O_2$)$^-$]$^+$, 10%), 220 ([M–($C_{11}H_{21}N_2O_2$)$^-$]$^+$, 17%). **HRMS** (ESI) calcd. for $C_{23}H_{29}{}^{37}ClFN_3O_2Na^+$ 458.18005 and $C_{23}H_{29}{}^{35}ClFN_3O_2Na^+$ 456.18300 ([M+Na]$^+$), found 458.17948, 456.18244. **IR** (film): ν_{max} 2972, 1701 (s), 1481, 1343 cm^{-1}. No spectroscopic data available for comparison.

1.5.20. Ethyl 4-((4-chloro-2-fluorophenyl)(pyridin-3-yl)methyl)-2,2-dimethylpiperazine-1-carboxylate, 20

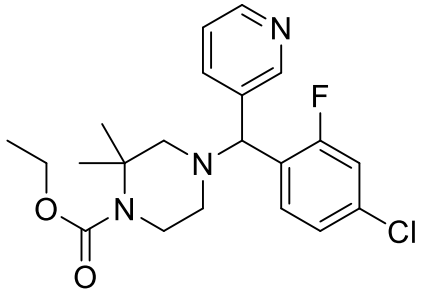

Prepared according to Method F, using TFA (2 mL, 27 mmol) and **19** (0.27 g, 0.66 mmol) in DCM (5 mL), anhydrous triethylamine (1.5 mL, 1.1 mmol), ethyl chloroformate (0.07 mL, 0.75 mmol). The crude product was purified with column chromatography (ethyl acetate/hexane) to give *the title compound* as an amber resin (40 mg, 15%). **^{1}H NMR** (600 MHz, Chloroform-*d*) δ 8.57 (m, 2H), 7.71 (dt, *J* = 8.0, 1.8 Hz, 1H), 7.54 (t, *J* = 8.0 Hz, 1H), 7.25 – 7.19 (m, 1H), 7.13 (dt, *J* = 8.4, 1.3 Hz, 1H), 7.02 (dd, *J* = 9.9, 2.1 Hz, 1H), 4.60 (s, 1H), 4.08 (q, *J* = 7.1 Hz, 2H), 3.65 – 3.24 (m, 2H), 2.78 – 2.29 (m, 2H), 2.27 – 1.92 (m, 2H), 1.39 (d, *J* = 2.1 Hz, 6H), 1.22 (t, *J* = 7.1 Hz, 3H). **^{13}C NMR** (151 MHz, Chloroform-*d*) δ 160.4 (d, *J* = 250.1 Hz), 157.0, 149.5, 149.0, 136.7, 135.5, 134.0 (d, *J* = 10.6 Hz), 129.3 (d, *J* = 4.6 Hz), 127.2 (d, *J* = 12.6 Hz), 125.3 (d, *J* = 3.4 Hz), 124.0, 116.7 (d, *J* = 25.9 Hz), 64.9, 64.1, 61.0, 55.2, 51.6, 42.8, 25.2, 24.8, 14.7. **LRMS** *m/z* (ESI) 430 ([M+Na]$^+$, 36%), 428 ([M+Na]$^+$, 100%), 408 ([M+H]$^+$, 7%), 406 ([M+H]$^+$, 16%). **HRMS** (ESI) calcd. for $C_{21}H_{25}{}^{37}ClFN_3O_2Na^+$ 430.14875 and $C_{21}H_{25}{}^{35}ClFN_3O_2Na^+$ 428.15170 ([M+Na]$^+$), found 430.14879, 428.15177. **IR** (film): ν_{max} 2974, 1701 (s), 1607, 1578, 1482, 1405, 1370, 1334 cm^{-1}. No spectroscopic data available for comparison.

1.5.21. *tert*-Butyl 4-((4-chloro-2-fluorophenyl)(pyridin-3-yl)methyl)-3-methylpiperazine-1-carboxylate, 21

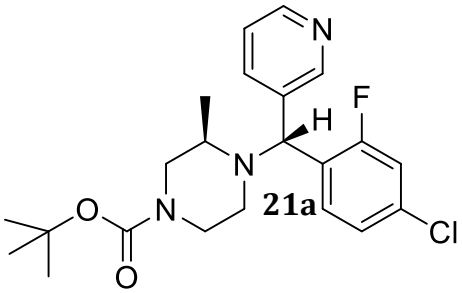

21a

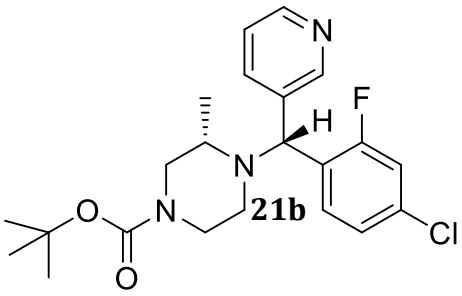

21b

Prepared according to Method E, using **14** (0.15 g, 0.6 mmol) and thionyl chloride (0.35 mL, 4.7 mmol), anhydrous triethylamine (0.7 mL, 5.1 mmol), dried potassium iodide (catalytic amount) and *tert*-butyl 3-methylpiperazine-1-carboxylate (0.19 g, 1.0 mmol) in anhydrous acetonitrile (4.5 mL) to give a crude orange oil. The crude oil was purified with column chromatography (ethyl acetate/hexane) to give two diastereomers of *the title compound* (**21a** and **21b**), and recovered **14** as a waxy brown solid (86 mg, 57%).

Isomer **20a** (57 mg, 22%) as a brown oil. **^{1}H NMR** (400 MHz, Chloroform-*d*) δ 8.66 (d, *J* = 2.1 Hz, 1H), 8.55 – 8.07 (m, 1H), 7.73 (dt, *J* = 8.0, 1.9 Hz, 1H), 7.38 (t, *J* = 8.0 Hz, 1H), 7.22 (dd, *J* = 7.9, 4.8 Hz, 1H), 7.09 (m, 2H), 5.16 (s, 1H), 3.70 (s, 1H), 3.58 – 3.44 (m, 1H), 3.30 (m, 1H), 3.15 (s, 1H), 2.86 (s, 1H), 2.52 (m, 1H), 2.26 (s, 1H), 1.43 (s, 9H), 1.02 (d, *J* = 6.4 Hz, 3H). **^{13}C NMR** (75 MHz, Chloroform-*d*) δ 160.4 (d, *J* = 249.5 Hz), 155.1, 149.6, 148.8, 137.4, 135.4, 134.0 (d, *J* = 10.6 Hz), 130.7 (d, *J* = 4.8 Hz), 125.8 (d, *J* = 13.9 Hz), 125.1 (d, *J* = 3.5 Hz), 123.7, 116.8 (d, *J* = 26.5 Hz), 79.7, 59.1, 50.2, 44.3, 28.5, 10.1 (2 obscured signals). **LRMS** *m/z* (ESI) 444 ([M+Na]$^+$, 36%), 442 ([M+Na]$^+$, 100%), 422 ([M+H]$^+$, 7%), 420 ([M+H]$^+$, 16%). **HRMS** (ESI) calcd. for $C_{22}H_{27}{}^{37}ClFN_3O_2Na^+$ 444.16440 and $C_{22}H_{27}{}^{35}ClFN_3O_2Na^+$ 442.16735 ([M+Na]$^+$), found 444.16379, 442.16670. **IR** (film): ν_{max} 2974, 1689 (s), 1603, 1574, 1478, 1423, 1379 cm^{-1}. No spectroscopic data available for comparison.

Isomer **20b** (61 mg, 23%) as a brown oil. **^{1}H NMR** (400 MHz, Chloroform-*d*) δ 8.64 (d, *J* = 2.1 Hz, 1H), 8.47 (dd, *J* = 4.8, 1.6 Hz, 1H), 7.92 – 7.56 (m, 2H), 7.23 (dd, *J* = 7.9, 4.8 Hz, 1H), 7.17 – 7.10 (m, 1H), 6.99 (dd, *J* = 10.0, 2.1 Hz, 1H), 4.96 (s, 1H), 4.33 – 3.46 (m, 2H), 3.41 – 2.75 (m, 3H), 2.77 – 2.29 (m, 2H), 1.43 (s, 9H),

0.94 (d, *J* = 6.5 Hz, 3H). **^{13}C NMR** (75 MHz, Chloroform-*d*) δ 160.4 (d, *J* = 250.0 Hz), 155.2, 149.8, 149.0, 135.9, 133.7 (d, *J* = 10.6 Hz), 129.0, 128.3 (d, *J* = 12.0 Hz), 125.2 (d, *J* = 3.6 Hz), 123.7, 116.6 (d, *J* = 25.8 Hz), 79.7, 60.1, 49.5, 43.5, 28.5, 8.4 (3 obscured signals). **LRMS** *m/z* (ESI) 444 ([M+Na]$^+$, 37%), 442 ([M+Na]$^+$, 100%), 422 ([M+H]$^+$, 3%), 420 ([M+H]$^+$, 12%). **HRMS** (ESI) calcd. for $C_{22}H_{27}{}^{37}ClFN_3O_2Na^+$ 444.16440 and $C_{22}H_{27}{}^{35}ClFN_3O_2Na^+$ 442.16735 ([M+Na]$^+$), found 444.16445, 442.16736. **IR** (film): ν_{max} 2967, 1692 (s), 1605, 1577, 1473, 1420, 1422, 1379 cm^{-1}. No spectroscopic data available for comparison.

1.5.22. Ethyl (*R*)-4-((*R*)-(4-chloro-2-fluorophenyl)(pyridin-3-yl)methyl)-3-methylpiperazine-1-carboxylate, 22a

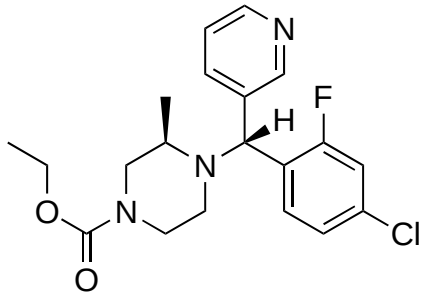

Prepared according to Method F, using TFA (1.5 mL, 20 mmol) and **21a** (52 mg, 0.12 mmol) in DCM (5 mL), anhydrous triethylamine (2 mL, 1.5 mmol), ethyl chloroformate (0.011 mL, 0.12 mmol). The crude product was purified with column chromatography (ethyl acetate/hexane) to give *the title compound* as an amber resin (11 mg, 25%). **^{1}H NMR** (400 MHz, Chloroform-*d*) δ 8.93 – 8.25 (m, 2H), 7.82 – 7.72 (m, 1H), 7.28 (d, *J* = 6.0 Hz, 2H), 7.17 – 6.97 (m, 2H), 5.20 (s, 1H), 4.44 – 4.00 (m, 2H), 3.84 – 3.06 (m, 3H), 3.01 – 1.83 (m, 4H), 1.23 (t, *J* = 7.1 Hz, 3H), 1.09 – 0.67 (m, 3H). **^{13}C NMR** (101 MHz, Chloroform-*d*) δ 160.5 (d, *J* = 250.1 Hz), 155.9, 153.9, 149.2, 148.5, 135.9, 130.8 (d, *J* = 4.8 Hz), 125.2, 124.0, 117.0 (d, *J* = 26.5 Hz), 61.5, 59.2, 50.3, 49.8, 44.4, 43.9, 14.8, 10.5 (2 obscured signals). **LRMS** *m/z* (ESI) 416 ([M+Na]$^+$, 41%), 414 ([M+Na]$^+$, 100%), 394 ([M+H]$^+$, 6%), 392 ([M+H]$^+$, 19%). **HRMS** (ESI) calcd. for $C_{20}H_{23}{}^{37}ClFN_3O_2Na^+$ 416.13310 and $C_{20}H_{23}{}^{35}ClFN_3O_2Na^+$ 414.13605 ([M+Na]$^+$), found 416.13322, 414.13608. **IR** (film): ν_{max} 2976, 1693 (s), 1606, 1577, 1481, 1429, 1382 cm^{-1}. No spectroscopic data available for comparison.

1.5.23. Ethyl (*S*)-4-((*R*)-(4-chloro-2-fluorophenyl)(pyridin-3-yl)methyl)-3-methylpiperazine-1-carboxylate, 22b

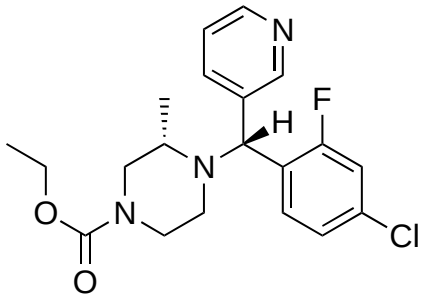

Prepared according to Method F, using TFA (1.5 mL, 20 mmol) and **21b** (56 mg, 0.13 mmol) in DCM (5 mL), anhydrous triethylamine (2 mL, 1.5 mmol), ethyl chloroformate (0.013 mL, 0.13 mmol). The crude product was purified with column chromatography (ethyl acetate/hexane) to give *the title compound* as an amber resin (17 mg, 34%). **^{1}H NMR** (400 MHz, Chloroform-*d*) δ 8.57 (m, 2H), 7.69 (m, 2H), 7.25 (dd, *J* = 7.6, 5.1 Hz, 1H), 7.15 (dd, *J* = 8.5, 2.1 Hz, 1H), 7.00 (dd, *J* = 10.0, 2.1 Hz, 1H), 4.98 (s, 1H), 4.12 (qq, *J* = 7.0, 3.6 Hz, 1H), 3.85 (m, 2H), 3.39 – 2.78 (m, 2H), 2.68 – 1.74 (m, 3H), 1.23 (t, *J* = 7.1 Hz, 3H), 1.05 – 0.89 (m, 3H). **^{13}C NMR** (101 MHz, Chloroform-*d*) δ 160.5 (d, *J* = 250.0 Hz), 156.1, 153.9, 149.7, 148.9, 136.1, 129.1, 125.4, 123.9, 116.7 (d, *J* = 25.8 Hz), 61.5, 60.2, 49.6, 43.8, 43.5, 14.8, 8.6 (3 obscured signals). **LRMS** *m/z* (ESI) 416 ([M+Na]$^{+}$, 38%), 414 ([M+Na]$^{+}$, 100%), 394 ([M+H]$^{+}$, 6%), 392 ([M+H]$^{+}$, 15%). **HRMS** (ESI) calcd. for $C_{20}H_{23}{}^{37}ClFN_3O_2Na^{+}$ 416.13310 and $C_{20}H_{23}{}^{35}ClFN_3O_2Na^{+}$ 414.13605 ([M+Na]$^{+}$), found 416.13320, 414.13611. **IR** (film): ν_{max} 2976, 1693 (s), 1606, 1578, 1480, 1427, 1382 cm^{-1}. No spectroscopic data available for comparison.

1.5.24. Cetirizine hydrochloride, 23

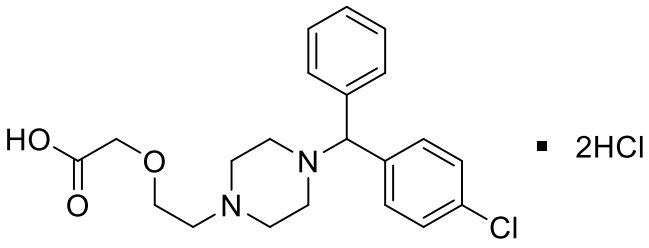

Purchased from Sigma Aldrich. **m.p.** 223.1–225.2˚C. **^{1}H NMR** (500 MHz, Deuterium Oxide) δ 7.63 – 7.59 (m, 2H), 7.58 – 7.44 (m, 5H), 7.45 – 7.37 (m, 2H), 5.38 (s, 1H), 4.24 (s, 2H), 4.07 – 3.83 (m, 2H), 3.72 (s, 4H), 3.58 – 3.52 (m, 2H), 3.49 (s, 4H). **^{13}C NMR** (126 MHz, Deuterium Oxide) δ 174.5, 135.1, 133.7, 132.6, 129.9, 129.8, 129.5, 127.9, 74.7, 67.5, 63.9, 55.9, 49.1, 48.3 (1 obscured signal). **LRMS** *m/z* (ESI) 413 ([M+Na]$^{+}$, 38%), 411 ([M+Na]$^{+}$, 100%), 391 ([M+H]$^{+}$, 28%), 389 ([M+H]$^{+}$, 76%), 203 ([M–($C_8H_{15}N_2O_3$)$^{-}$]$^{+}$, 15%), 201 ([M–($C_8H_{15}N_2O_3$)$^{-}$]$^{+}$, 40%). **HRMS** (ESI) calcd. for $C_{21}H_{26}{}^{37}ClN_2O_3^{+}$ 391.16025 and $C_{21}H_{26}{}^{35}ClN_2O_3^{+}$ 389.16320 ([M+H]$^{+}$), found 391.15987, 389.16286. Spectroscopic data matched those in the literature.[56-57]

References

1. WHO: Mycetoma. http://www.who.int/buruli/mycetoma/en/ (accessed 09/05/2017).

2. Zijlstra, E. E.; van de Sande, W. W. J.; Welsh, O.; Mahgoub, E. S.; Goodfellow, M.; Fahal, A. H., Mycetoma: a unique neglected tropical disease. *The Lancet Infectious Diseases* **2016,** *16* (1), 100–112.

3. Hassan, F. A., *Mycetoma — Clinicopathological Monograph*. Khartoum University Press: Khartoum, 2006; p 112.

4. El-Hassan, A. M.; Mahgoub, E. S., Lymph node involvement in mycetoma. *Trans. R Soc. Trop. Med. Hyg.* **1972,** *66* (1), 165–169.

5. Fahal A. H., A. M. A. R., El-Hassan A. M., Aggressive clinical presentation of Mycetoma due to Actinomadura Pelletierii. *Khartoum Medical Juornal* **2012,** *5* (1), 699–702.

6. Neglected tropical diseases. http://www.who.int/neglected_diseases/diseases/en/ (accessed 09/05/2017).

7. van de Sande, W. W. J.; Maghoub, E. S.; Fahal, A. H.; Goodfellow, M.; Welsh, O.; Zijlstra, E., The Mycetoma Knowledge Gap: Identification of Research Priorities. *PLOS Neglected Tropical Diseases* **2014,** *8* (3), e2667.

8. Lopez-Martinez, R.; Mendez-Tovar, L. J.; Bonifaz, A.; Arenas, R.; Mayorga, J.; Welsh, O.; Vera-Cabrera, L.; Padilla-Desgarennes, M. C.; Contreras Perez, C.; Chavez, G.; Estrada, R.; Hernandez-Hernandez, F.; Manzano-Gayosso, P., Update on the epidemiology of mycetoma in Mexico. A review of 3933 cases. *Gaceta medica de Mexico* **2013,** *149* (5), 586–592.

9. Kloezen, W.; van Helvert-van Poppel, M.; Fahal, A. H.; van de Sande, W. W. J., A Madurella mycetomatis Grain Model in Galleria mellonella Larvae. *PLOS Neglected Tropical Diseases* **2015,** *9* (7), e0003926.

10. FDA Drug Safety Communication: FDA limits usage of Nizoral (ketoconazole) oral tablets due to potentially fatal liver injury and risk of drug

interactions and adrenal gland problems. https://www.fda.gov/drugs/drugsafety/ucm362415.htm (accessed 09/05/2017).

11. Fahal, A. H.; Rahman, I. A.; El-Hassan, A. M.; Rahman, M. E.; Zijlstra, E. E., The safety and efficacy of itraconazole for the treatment of patients with eumycetoma due to Madurella mycetomatis. *Trans. R Soc. Trop. Med. Hyg.* **2011,** *105* (3), 127–132.

12. DNDi: About Mycetoma. https://www.dndi.org/diseases-projects/mycetoma/ (accessed 05/09/2017).

13. DNDi: Mycetoma – Disease Background. https://www.dndi.org/diseases-projects/mycetoma/mycetoma-disease-background/ (accessed 09/05/2017).

14. DNDi: Fosravuconazole. https://www.dndi.org/diseases-projects/portfolio/fosravuconazole/ (accessed 09/05/2017).

15. Duffy, S.; Sykes, M. L.; Jones, A. J.; Shelper, T. B.; Simpson, M.; Lang, R.; Poulsen, S. A.; Sleebs, B. E.; Avery, V. M., Screening the medicines for Malaria Venture Pathogen Box across multiple pathogens reclassifies starting points for open-source drug discovery. *Antimicrob. Agents Chemother.* **2017,** *61* (9).

16. Keenan, M.; Abbott, M. J.; Alexander, P. W.; Armstrong, T.; Best, W. M.; Berven, B.; Botero, A.; Chaplin, J. H.; Charman, S. A.; Chatelain, E.; von Geldern, T. W.; Kerfoot, M.; Khong, A.; Nguyen, T.; McManus, J. D.; Morizzi, J.; Ryan, E.; Scandale, I.; Thompson, R. A.; Wang, S. Z.; White, K. L., Analogues of fenarimol are potent inhibitors of Trypanosoma cruzi and are efficacious in a murine model of Chagas Disease. *J. Med. Chem.* **2012,** *55* (9), 4189–4204.

17. Kepler, T. B.; Marti-Renom, M. A.; Maurer, S. M.; Rai, A. K.; Taylor, G.; Todd, M. H., Open source research the power of us. *Aust. J. Chem.* **2006,** *59* (5), 291-294.

18. Munos, B., Can open-source R&D reinvigorate drug research? *Nat Rev Drug Discov* **2006,** *5* (9), 723-729.

19. Williamson, A. E.; Ylioja, P. M.; Robertson, M. N.; Antonova-Koch, Y.; Avery, V.; Baell, J. B.; Batchu, H.; Batra, S.; Burrows, J. N.; Bhattacharyya, S.; Calderon, F.; Charman, S. A.; Clark, J.; Crespo, B.; Dean, M.; Debbert, S. L.; Delves, M.; Dennis, A.

S. M.; Deroose, F.; Duffy, S.; Fletcher, S.; Giaever, G.; Hallyburton, I.; Gamo, F.-J.; Gebbia, M.; Guy, R. K.; Hungerford, Z.; Kirk, K.; Lafuente-Monasterio, M. J.; Lee, A.; Meister, S.; Nislow, C.; Overington, J. P.; Papadatos, G.; Patiny, L.; Pham, J.; Ralph, S. A.; Ruecker, A.; Ryan, E.; Southan, C.; Srivastava, K.; Swain, C.; Tarnowski, M. J.; Thomson, P.; Turner, P.; Wallace, I. M.; Wells, T. N. C.; White, K.; White, L.; Willis, P.; Winzeler, E. A.; Wittlin, S.; Todd, M. H., Open Source Drug Discovery: Highly potent antimalarial compounds derived from the tres cantos arylpyrroles. *ACS Central Science* **2016,** *2* (10), 687-701.

20. Woelfle, M.; Olliaro, P.; Todd, M. H., Open science is a research accelerator. *Nat Chem* **2011,** *3* (10), 745-748.

21. Paul, S. M.; Mytelka, D. S.; Dunwiddie, C. T.; Persinger, C. C.; Munos, B. H.; Lindborg, S. R.; Schacht, A. L., How to improve R&D productivity: the pharmaceutical industry's grand challenge. *Nat Rev Drug Discov* **2010,** *9* (3), 203-214.

22. Maurer, S. M.; Rai, A.; Sali, A., Finding cures for tropical diseases: Is open source an answer? *PLOS Medicine* **2005,** *1* (3), e56.

23. Balasegaram, M.; Kolb, P.; McKew, J.; Menon, J.; Olliaro, P.; Sablinski, T.; Thomas, Z.; Todd, M. H.; Torreele, E.; Wilbanks, J., An open source pharma roadmap. *PLOS Medicine* **2017,** *14* (4), e1002276.

24. Eisch, J. J., Henry Gilman: American pioneer in the rise of organometallic chemistry in modern science and technology. *Organometallics* **2002,** *21* (25), 5439-5463.

25. Cahiez, G.; Alami, M.; Taylor, R. J. K.; Reid, M.; Foot, J. S.; Fader, L.; Sikervar, V.; Pabba, J., Manganese Dioxide. In *Encyclopedia of Reagents for Organic Synthesis*, John Wiley & Sons, Ltd: 2001.

26. Weissman, S. A.; Zewge, D.; Chen, C., Ligand-free palladium-catalyzed cyanation of aryl halides. *J. Org. Chem.* **2005,** *70* (4), 1508–1510.

27. Burchat, A. F.; Chong, J. M.; Nielsen, N., Titration of alkyllithiums with a simple reagent to a blue endpoint. *J. Org. Chem.* **1997,** *542* (2), 281-283.

28. Gessner, V. H.; Däschlein, C.; Strohmann, C., Structure formation principles and reactivity of organolithium compounds. *Chemistry – A European Journal* **2009,** *15* (14), 3320-3334.

29. Rathman, T. L.; Bailey, W. F., Optimization of organolithium reactions. *Org. Process Res. Dev.* **2009,** *13* (2), 144-151.

30. Smith, M.; March, J., March's advanced organic chemistry: reactions, mechanisms, and structure. 6th ed.; Wiley-Interscience: Hoboken, N.J, 2007.

31. Schlosser, M., *Organometallics in synthesis: a manual*. Wiley: New York;Chichester, West Sussex, England;, 1994.

32. Kuhn, D. D.; Young, T. C., Photolytic degradation of hexacyanoferrate (II) in aqueous media: The determination of the degradation kinetics. *Chemosphere* **2005,** *60* (9), 1222-1230.

33. Bickerton, G. R.; Hopkins, A. L., Drug discovery. Know your chemical space. *Nat. Chem. Biol.* **2010,** *6* (7), 482-483.

34. Kobayashi, K.; Shiokawa, T.; Omote, H.; Hashimoto, K.; Morikawa, O.; Konishi, H., New synthesis of isoquinoline and 3,4-dihydroisoquinoline derivatives. *Bull. Chem. Soc. Jpn.* **2006,** *79*, 1126-1132.

35. Brown, A. C.; Gibson, J., XXX.-A rule for determining whether a given benzene mono-derivative shall give a meta-di-derivative or a mixture of ortho- and para-di-derivatives. *J. Chem. Soc. Faraday Trans.* **1892,** *61* (0), 367-369.

36. Otero, N.; Mandado, M.; Mosquera, R. A., Nucleophilicity of indole derivatives: activating and deactivating effects based on proton affinities and electron density properties. *J. Phys. Chem* **2007,** *111* (25), 5557.

37. Knepper, I.; Seichter, W.; Skobridis, K.; Theodorou, V.; Weber, E., Aspects of crystal engineering arising from packing behavior of functional mono para-substituted trityl compounds. *CrystEngComm* **2015,** *17* (33), 6355-6369.

38. Stabile, R. G.; Dicks, A. P., Semi-microscale Williamson ether synthesis and simultaneous isolation of an expectorant from cough tablets. *J. Chem. Educ.* **2003,** *80* (3), 313.

39. Chen, X.; Brauman, J. I., Hydrogen bonding lowers intrinsic nucleophilicity of solvated nucleophiles. *J. Am. Chem. Soc.* **2008,** *130* (45), 15038-15046.

40. Peters, K. S., Nature of dynamic processes associated with the SN1 reaction mechanism. *Chemical Reviews* **2007,** *107* (3), 859-873.

41. Bissinger, W. E.; Kung, F. E., A study of the reaction of alcohols with thionyl chloride1. *J. Am. Chem. Soc.* **1947,** *69* (9), 2158-2163.

42. Nutaitis, C. F.; Gribble, G. W., Reactions of sodium borohydride in acidic media. XIV. Reductive cleavage of cyclic acetals and ketals to hydroxyalkyl ethers. *Org. Prep. Proc. Int.* **1985,** *17* (1), 11-16.

43. Gribble, G. W.; Leese, R. M.; Evans, B. E., Reactions of sodiurn borohydride in acidic media; IV. Reduction of diarylmethanols and triarylmethanols in trifluoroacetic acid1-3. *Synthesis* **1977,** *1977* (03), 172-176.

44. Keenan, M.; Alexander, P. W.; Diao, H.; Best, W. M.; Khong, A.; Kerfoot, M.; Thompson, R. C.; White, K. L.; Shackleford, D. M.; Ryan, E.; Gregg, A. D.; Charman, S. A.; von Geldern, T. W.; Scandale, I.; Chatelain, E., Design, structure-activity relationship and in vivo efficacy of piperazine analogues of fenarimol as inhibitors of Trypanosoma cruzi. *Bioorganic Med. Chem.* **2013,** *21* (7), 1756-63.

45. Khalili, F.; Henni, A.; East, A. L., pKa values of some piperazines at (298, 303, 313, and 323) K. *J. Chem. Eng. Data* **2009,** *54* (10), 2914-2917.

46. Linnell, R., Notes- Dissociation constants of 2-substituted pyridines. *J. Org. Chem.* **1960,** *25* (2), 290-290.

47. Schrödinger, E., An undulatory theory of the mechanics of atoms and molecules. *Physical Review* **1926,** *28* (6), 1049-1070.

48. Pietronero, L.; Zirilli, F., Limitations and validity of the Hartree--Fock method. *Nuovo Cim.* **1974**, 57-62.

49. Combes, J.-M.; Duclos, P.; Seiler, R., The born-oppenheimer approximation. In *Rigorous atomic and molecular physics*, Springer: 1981; pp 185-213.

50. Froese Fischer, C., General Hartree-Fock program. *Comput. Phys. Commun.* **1987,** *43* (3), 355-365.

51. Neel, A. J.; Hilton, M. J.; Sigman, M. S.; Toste, F. D., Exploiting non-covalent [pi] interactions for catalyst design. *Nature* **2017,** *543* (7647), 637.

52. Willcott, M. R., MestRe Nova. *J. Am. Chem. Soc.* **2009,** *131* (36), 13180-13180.

53. Payne, D. J.; Gwynn, M. N.; Holmes, D. J.; Pompliano, D. L., Drugs for bad bugs: confronting the challenges of antibacterial discovery. *Nat Rev Drug Discov* **2007,** *6* (1), 29-40.

54. Moffat, J. G.; Vincent, F.; Lee, J. A.; Eder, J.; Prunotto, M., Opportunities and challenges in phenotypic drug discovery: an industry perspective. *Nat Rev Drug Discov* **2017,** *16* (8), 531-543.

55. Smit, S.; Derks, M. F. L.; Bervoets, S.; Fahal, A.; van Leeuwen, W.; van Belkum, A.; van de Sande, W. W. J., Genome sequence of Madurella mycetomatis mm55, isolated from a human mycetoma case in sudan. *Genome Announcements* **2016,** *4* (3), e00418-16.

56. Dyakonov, T.; Muir, A.; Nasri, H.; Toops, D.; Fatmi, A., Isolation and characterization of cetirizine degradation product: Mechanism of Cetirizine Oxidation. *Pharmaceutical Research* **2010,** *27* (7), 1318-1324.

57. Tan, Z.-R.; Ouyang, D.-S.; Zhou, H.-H.; Zhou, G.; Wang, L.-S.; Wang, D.; Li, Z., Sensitive bioassay for the simultaneous determination of pseudoephedrine and cetirizine in human plasma by liquid-chromatography–ion trap spectrometry. *J. Pharm. Biomed. Anal.* **2006,** *42* (2), 207-212.